https://doi.org/10.5194/hess-2021-558
Preprint. Discussion started: 8 November 2021

Hydrology and Earth System Sciences
Discussions
Open Access

Soil water sources in permafrost active layer of Three-River Headwater Region, China

Li Zongxing[1], Gui Juan[1], Zhang Baijuan[1], Feng Qi[1]

1.Key Laboratory of Ecohydrology of Inland River Basin/Gansu Qilian Mountains Eco-Environment Research Center, Northwest Institute of Eco-Environment and Resources, Chinese Academy of Sciences, Lanzhou 730000, China

Abstract:

Water in permafrost soil is an important factor affecting the ecology of cold environments, climate change, hydrological cycle, engineering, and construction. To explore the variations in soil water in the active layer due to permafrost degradation, the soil water sources in the Three-River Headwater Region were quantified based on the stable isotope data (δ^2H and $\delta^{18}O$) of 1140 samples. The results showed that the evaporation equation was $\delta^2H = 7.46\ \delta^{18}O - 0.37$ for entire soil water. The stable isotope data exhibited a spatial pattern, which varied over the soil profile under the influence of altitude, soil moisture, soil temperature, vegetation, precipitation infiltration, soil water movement, ground ice, and evaporation. Based on the stable isotope tracer model, precipitation and ground ice accounted for approximately 88% and 12% of soil water, respectively. High precipitation contributed to the soil water in the 3900–4100 m, 4300–4500 m, and 4700–4900 m zones, whereas ground ice contributed to the soil water in the 4500–4700 m and 4900–5100 m zones. Precipitation contributed approximately 84% and 80% to the soil water in grasslands and meadows, respectively, whereas ground ice contributed approximately 16% and 20%, respectively. Precipitation; evapotranspiration; physical and chemical properties of soil; and the

https://doi.org/10.5194/hess-2021-558
Preprint. Discussion started: 8 November 2021

Hydrology and Earth System Sciences Discussions
Open Access

distribution of ground ice, vegetation, and permafrost degradation were the major factors affecting the soil water sources in the active layer. Therefore, establishing an observation network and developing technologies for ecosystem restoration and conservation is critical to effectively mitigate ecological problems caused by future permafrost degradation in the study region.

Key words: soil water sources, permafrost active layer, stable isotopes, Three-river Headwaters Region

1. Introduction

Soil water is the critical element of the water cycle and is closely associated with precipitation, surface water, groundwater, and plant water (Sprenger et al., 2016). Being an important link between the cryosphere, atmosphere, biosphere, hydrosphere, and lithosphere, soil water is a key factor in ground–air exchange, land surface processes, and hydrological processes in alpine regions (Tan et al., 2017). In addition, soil water holds most of the information pertaining to surface hydrological processes. It influences the infiltration and runoff ratios of rainfall and evaporation and controls the distribution of water and energy (Jean et al., 1998). The evolution of soil water is primarily controlled by external factors, such as precipitation, temperature, solar radiation, runoff, surface evapotranspiration, and human activities, as well as internal factors, such as vegetation, topography, altitude, soil type, physical and chemical properties of soil, and soil particle characteristics. Moreover, soil water has a significant effect on local and global climate by altering surface albedo, surface heat capacity, and latent and sensible heat turbulence fluxes. Seasonal variations in soil water can directly or indirectly affect

https://doi.org/10.5194/hess-2021-558
Preprint. Discussion started: 8 November 2021

plant physiological metabolic processes, change the distribution of elemental contents in plants, and alter plant resource acquisition strategies and biomass distribution patterns, thereby affecting the community structure and species diversity of the ecosystem (Liu et al., 2021).

Stable isotope tracing has recently emerged as a new approach for studying the water cycle, overcoming the limitations of traditional methods to expand research on soil water (Brooks et al., 2015; Sprenger et al., 2016; Li et al., 2020). "Araguás-Araguás et al. (1995) revealed that extracted soil water was depleted in δ^2H and $\delta^{18}O$ by 5–10‰ and 0.3–0.5‰, respectively, and that these depletions were strongly dependent on the soil type. The enrichment of heavy isotopes in topsoil has reportedly followed a seasonal hysteresis pattern, thereby indicating a lag time between the fractionation signal in soil and the increase/decrease in soil evaporation in spring/autumn (Sprenger et al., 2017). Tan et al. (2017) also reported that the $\delta^{18}O$ and δ^2H values of soil water varied with season and soil profile depth. The seasonal variations in soil profiles also differed between wet and dry years. Che et al. (2019) revealed considerable variations in the $\delta^{18}O$ value of soil water in shallow soil due to evaporation and precipitation infiltration, whereas it was less affected by these factors in the middle and deep soil layers. The spatial characteristics of stable isotopes in soil water are manifested by the fluctuations in the vertical soil profile (Gaj et al., 2016). Based on stable isotope tracing, Wu et al. (2017) observed the evaporation front in the 5–10 cm soil layer, and water vapor exchange motions occurred in the 0–5 cm soil layer before it diffused to the outside. They also revealed that approximately 4.5% of soil water in the 0–20 cm soil layer was evaporated during the maize-growing season, and 72.6% of the evaporated vapor was condensed. Liu et al. (2011) confirmed that

https://doi.org/10.5194/hess-2021-558
Preprint. Discussion started: 8 November 2021

Hydrology and Earth System Sciences
Discussions

subalpine non-phreatophytic shrubs primarily consumed soil water from the upper 30 cm of the soil profile and revealed that water uptake patterns were positively correlated with the rootlet biomass distribution and soil water content. The significant differences in $\delta^{18}O$ and $\delta^{2}H$ values between root water and soil water are likely associated with isotopic fractionation during root water uptake, leaf surface water pools, and ecohydrological separation (Liu et al., 2021). Through stable isotope tracing, Carey and Feng (2004) revealed the mixing and preferential flow paths of soil water. Water from a small rainfall event (approximately 4.0 mm/d) also penetrated the soil to the depths of 40–50 cm, and the mean effective contribution of soil recharge (0–50 cm deep) occurred after 3–5 d despite the occurrence of large precipitation events (15.0–18.9 mm/d) (Liu et al., 2015). The seasonal variations in stable isotopes in soil water reflect the mixing of old and new soil water and the process of transport and redistribution, which is primarily caused by precipitation, temperature, and seasonal variations in plant growth (Klaus and McDonnell, 2013). However, little research has been conducted on the soil water sources in the permafrost active layer.

Being a crucial element of the cryosphere, permafrost plays an important role in ground–air exchange, surface processes, and hydrological cycle. The permafrost active layer acts as a “buffer layer” between permafrost and atmosphere; thus, it is a transition layer for water and heat exchange. Soil water in permafrost is an important factor affecting the ecology of cold environments, climate change, engineering, and construction (Guo et al., 2002). Under the influence of global warming and human activities, permafrost degradation has gradually changed the soil water process on the Qinghai–Tibet Plateau. This has resulted in environmental problems (such as land desertification, grassland degradation/sanding, and reduced biodiversity) and the

https://doi.org/10.5194/hess-2021-558
Preprint. Discussion started: 8 November 2021

degradation of ecosystem function, thereby weakening the role of ecological barriers and posing a serious threat to natural ecological security (Chen et al., 2012).

The Three-River Headwater Region is the study area in this research because it is currently undergoing permafrost degradation due to global warming. Based on the 1140 samples of soil water, precipitation, river water, ground ice, supra-permafrost water, and glacier snow meltwater collected from June 2019 to July 2020, this study (a) analyzes the spatiotemporal distribution of δ^2H and δ^{18}O in soil water; (b) discusses the influencing factors and hydrological processes of soil water in the permafrost active layer; (c) explores the major sources of (and contributions to) soil water; and (d) confirms the corresponding implications for ecological protection. This study provides a scientific basis for establishing soil parameters in hydrological models, thereby providing technical support for predicting the evolution of water resources under permafrost degradation. Moreover, it provides a theoretical basis for developing ecological protection and vegetation restoration models in cold regions.

2. Data and methods

2.1 Study region

The Three-River Headwater Region is located in the core region of the “two screens and three belts” national ecological barrier in China, representing one of the key ecological function regions (Fig. 1). It is a habitat of unique and rare wildlife on the Qinghai–Tibet Plateau with highest biodiversity. It is also an important site for constructing ecological civilization. The first largest national park, the Three-River Headwater National Park, was constructed in this region. Being the headwater area of the Yangtze, Yellow, and Lancangjiang rivers (Fig. 1), it is an important recharge area for freshwater resources and a water

https://doi.org/10.5194/hess-2021-558
Preprint. Discussion started: 8 November 2021

conservation region for China and the surrounding areas and is known as the "Chinese Water Tower" and the "Source of Life." The Three-River Headwater Region covers 363,000 km^2 (31°39'–36°12'E, 89°45'–102°23'E), accounting for 50.4% of the total area of Qinghai Province. The landscape is predominantly mountainous with complex topography and altitudes ranging from 3335 m to 6564 m. The climate is typically alpine continental, with cold and hot seasons, dry and wet seasons, a small annual temperature difference, a large daily temperature difference, long sunshine hours, and strong radiation with no evident seasonal variation. The source regions of the Yellow, Yangtze, and Lancangjiang rivers cover 167,000 km^2, 159,000 km^2, and 37,000 km^2, accounting for 46%, 44%, and 10% of the total area of the study region, respectively. The source regions of the Yellow, Yangtze, and Lancangjiang rivers contribute approximately 49%, 25%, and 15% of the total runoff, respectively, and supply up to 60 × 10^9 m^3/a of freshwater resources. Additionally, more than 180 rivers, 1800 lakes, 200 × 10^9 m^3 of glaciers, and 73,300 km^2 of wetlands are present in the Three-River Headwater Region.

The ecosystems in the Three-River Headwater Region are characterized by diversity, fragility, sensitivity, weak carrying capacity, and restoration capacity. Grasslands are structurally disordered and dysfunctional, and forests and scrubs have a homogeneous composition and a weak regeneration capacity. Wetlands are poorly regulated and have a weak restoration ability. Desert areas have a simple structural hierarchy, low vegetation cover, low species composition, and poor stability. Under the influence of global warming, the study region has been experiencing glacier retreat, permafrost degradation, increasing precipitation, decreasing snowfall, declining water conservation, and intensified soil erosion. These changes have caused large variations in soil water, leading

https://doi.org/10.5194/hess-2021-558
Preprint. Discussion started: 8 November 2021

to considerable uncertainty regarding vegetation growth and major difficulties in vegetation and ecological restoration in permafrost regions. Therefore, studying the soil water sources in the permafrost active layer is necessary to improve the effectiveness of ecological restoration.

2.2 Collection and preparation of samples

Observing ecohydrological processes on the Qinghai–Tibet Plateau is difficult because of the harsh natural conditions (Li et al., 2020), and thus, the dominant contributor to soil water remains largely unknown. Hence, samples from various waterbodies in the Three-River Headwater Region were systematically sampled for the first time in this study; the samples included soil water, ground ice, precipitation, river water, supra-permafrost water, and glacier snow meltwater. A total of 1140 samples were collected between June 2019 and July 2020 at continuous spatial and temporal frequencies (Fig. 1). The sampling details are described below.

Soil samples: In July 2019, soil profiles of 1 m were excavated at 90 sampling sites. Triplicate samples were collected at intervals of 20 cm for the stable isotopic analysis of soil water. The samples were collected from 1 cm below the surface to avoid the influence of the free atmosphere on the soil samples. A total of 450 soil samples were collected, each of which was immediately placed in a high density polyethylene (HDPE) bottle and sealed with parafilm before being transported to the laboratory for refrigeration. Soil water and temperature were simultaneously measured during sampling using a portable soil water measurement instrument (TZS-IW) (Fig. 1). Soil temperature ranged from -40 ℃ to 100 ℃ with an accuracy of ± 0.5 ℃. Soil moisture (% (m^3/m^3)) ranged between 0–100% with a response time of < 2 s.

Precipitation samples: A total of 375 precipitation (event scale) samples were collected from five stations at different altitudes from June

https://doi.org/10.5194/hess-2021-558
Preprint. Discussion started: 8 November 2021

2019 to July 2020: Zhimenda (92.26° E, 34.14° N, 3540 m), Tuotuohe (34.22° N, 92.24° E, 4533 m), Zaduo (32.53° N, 95.17° E, 4066.4 m), Dari (33.45° N, 99.39° E, 3967 m), and Maduo (34.55° N, 98.13° E, 4272.3 m) (Fig. 1). Precipitation, air temperature, wind speed, and relative humidity were recorded during sample collection at the corresponding national meteorological stations. Precipitation occurring from 20:00 on the first day to 20:00 the next day was collected to sample a precipitation event. To avoid evaporation, samples were collected immediately after the event. Before installing the collectors, the funnels and flasks were carefully cleaned and dried. After each precipitation event, the collected rainwater or snow was loaded into pre-cleaned HDPE sample bottles sealed with parafilm.

Ground ice: Collecting ground ice samples, can be challenging, particularly during the ablation period. At each sampling sites, a 1 m deep profile was dug in the permafrost active layer for frozen ground ice (Fig. 2). The outer layer of ice samples was chipped off to avoid soil contamination. Ground ice samples were preserved in pre-cleaned HDPE bottles sealed with parafilm and stored frozen. A total of 41 ground ice samples were obtained at different altitudes in the study region.

River water: To analyze the spatiotemporal characteristics of stable isotopes of soil water and river water, river water samples were collected from the main stream (32 samples) and major tributary (125 samples) during July 2019. The samples were collected at a depth of 20 cm below the water surface and stored in HDPE bottles sealed with parafilm.

Supra-permafrost water: Supra-permafrost water is the most widely distributed groundwater in the study area and is primarily stored in the permafrost active layer (Li et al., 2020). To analyze the spatiotemporal patterns of stable isotopes in supra-permafrost water and the hydraulic connection between supra-permafrost water and soil water, 94 supra-permafrost water samples were collected at different altitudes during July 2019. Sampling was performed manually by digging a profile of 1 m depth in the permafrost active layer at each sampling site. The water samples collected from the bottom of each profile were immediately filtered through a 0.45-μm Millipore filters before being stored in HDPE bottles sealed with parafilm.

Glacier snow meltwater: In July 2019, 23 samples were collected from streams flowing out of the glacier fronts at Jianggudiru Glacier (91° E, 33.45° N, 5281 m), Dongkemadi Glacier (92° E, 33° N, 5423 m), and Yuzhufeng Glacier (94.22° E, 35.63° N, 5180 m) in the source region of the Yangtze River (Fig. 1); Halong Glacier (99.78° E, 34.62° N, 5050 m) in the source region of the Yellow River; and Yangzigou Glacier (94.85° E, 33.46° N, 5260 m) in the source region of the Lancangjiang River. The samples were stored in HDPE bottles sealed with parafilm.

Measurement of δ^2H and $\delta^{18}O$: For the analysis of δ^2H and $\delta^{18}O$, water was extracted from soil using a cryogenic freezing vacuum extraction system (LI-2000, Beijing Liga United Technology Co., Ltd., China), which can achieve complete extraction with high precision (Li et al., 2016). Test tubes containing soil samples were installed on the extraction line and frozen in liquid nitrogen. After 10 min, the line was checked to ensure that there were no leaks. After completely sealing it, the larger test tube was heated to 95 °C using a heating sleeve, and the smaller test tube was frozen with liquid nitrogen (-196 ºC). Water vapor moved from the larger test tube to the smaller one and condensed to ice owing to the temperature gradient. The extraction process required 2 h and had an efficiency of > 98%. Before analysis, all samples were stored in a refrigerator at 4 ºC without evaporation. Water samples were analyzed for $\delta^{18}O$ and δ^2H via laser absorption spectroscopy (liquid water isotope analyzer, Los Gatos Research DEL-100, USA) at the Key

https://doi.org/10.5194/hess-2021-558
Preprint. Discussion started: 8 November 2021

Laboratory of Ecohydrology of Inland River Basin, Northwest Institute of Eco-Environment and Resources, Chinese Academy of Sciences. The results were reported relative to the Vienna Standard Mean Ocean Water. The measurement precisions for $\delta^{18}O$ and $\delta^{2}H$ were better than 0.5‰ and 0.2 ‰, respectively.

2.3 Methods

The global meteoric water line (GMWL) can be determined by analyzing the relationship between the $\delta^{18}O$ and $\delta^{2}H$ values of different waterbodies worldwide (Craig, 1961). The slope and intercept of local meteoric water lines (LMWLs) in different regions typically deviate from the GMWL. The evaporation line (EL) can also be obtained from the regression analysis of soil water isotope data in an open liquid–gas isotope system (Landwehr and Stewart, 2014). By calculating the effect of the LMWL on evaporation, the line-conditioned excess (lc-excess) can be determined as follows (Landwehr and Coplen, 2006):

$$\text{lc-excess} = \delta^{2}H - a \times \delta^{18}O - b \qquad (1)$$

where a and b represent the slope and intercept of the LMWL, respectively.

The end member mixing analysis (EMMA) tracer approach has been widely used for analyzing potential water sources contributing to streamflow (Hooper et al., 1990; Hooper, 2003; Gibson et al., 2005; Peng et al., 2012; Li et al., 2014, 2020). The EMMA tracer method assumes that i) the tracer concentration in a potential water source varies significantly in time and space, ii) chemical properties of the selected tracer are stable, and iii) changes occur as a result of water mixing. Tracer techniques involve graphical analyses in which chemical and isotopic parameters represent the designated endmembers. Essentially, the changing composition of the studied water likely results from the intersections during its passage through each landscape. Tracers can be

https://doi.org/10.5194/hess-2021-558
Preprint. Discussion started: 8 November 2021

used to determine the sources and flow paths. Both the two- and three-component methods can be described by a uniform equation:

$$Q_t = \sum_{m=1}^{n} Q_m, \quad Q_t C_t^j = \sum_{m=1}^{n} Q_m C_m^j, \; j = l,\ldots,k \quad (2)$$

where Q_t is the total runoff discharge, Q_m is the discharge of component *m*, and C^m_j is the tracer *j* incorporated in the component *m*. For isotope hydrograph separation, one of the tracers should be an isotope. If there are more than four endmembers, calculation software, such as IsoSource, must be used (Phillips and Gregg, 2003).

3. Results

3.1 Relationship between $\delta^{18}O$ and δ^2H in soil water

In the Three-River Headwater Region, the mean $\delta^{18}O$ value was -11.58‰ (ranging from -20.86‰ to -0.74‰) and the mean d-excess was 5.77‰ (ranging from -15.41‰ to 54.50‰). Regional differences were observed, whereby the mean values of $\delta^{18}O$ and d-excess were -10.14‰ (-19.71‰ to -4.82‰) and 6.89‰ (-11.98‰ to 24.46‰), respectively, in the source regions of the Yangtze River, -11.66‰ (-18.56‰ to -0.74‰) and 5.4‰ (-15.41‰ to 18.85‰), respectively, in the source region of the Yellow River, and -14.65‰ (-20.86‰ to -7.57‰) and 4.62‰ (-8.05‰ to 13.91‰), respectively, in the source region of the Lancangjiang River. Based on the regression analyses of all the stable isotope data of soil water, the EL was determined to be $\delta^2H = 7.46\ \delta^{18}O - 0.37$ ($R^2 = 0.94$, $p < 0.01$) for the entire study area (Fig. 3). The low slope, particularly the negative intercept, indicates that soil water was strongly affected by evaporation or non-equilibrium dynamic fractionation. In addition, the EL varied with soil layers, and the slope and intercept were similar between the 0–20 cm and 20–40 cm soil layers. The EL evidently decreased in the following order: 40–60 cm, 60–80 cm, and 80–100 cm soil layers, which may be explained by three reasons as follows. (1) Different water sources or supply proportions of soil water. The soil water in the upper layers may have been predominantly contributed by recent precipitation with relatively negative stable isotopes, whereas the deeper soil layers may have been more affected by "old" soil water with relatively positive stable isotopes. (2) The difference in the evaporation intensity of soil water. The effect of evaporation gradually decreases from the top to the bottom of the soil profile; however, the evaporation-affected soil water continues to migrate toward the bottom through piston flow, thereby changing the isotopic composition of soil water. (3) The influences of soil hydrological processes, including precipitation infiltration (preferential or piston flow), vegetation root uptake, soil water movement, and soil texture. Under different climates, altitudes, vegetation types, and geomorphology, the slope and intercept of EL were ranked as follows: source region of the Yangtze River > source region of the Lancangjiang River > source region of the Yellow River (Fig. 3b).

In addition, a negative correlation was observed between the $\delta^{18}O$ and d-excess values of soil water in the study area (Table 1). However, the correlation coefficients were not significant, indicating the multiplicity and complexity of the evolution of stable isotopes in soil water. Interestingly, the correlation coefficient increased from the top to the bottom of the soil profile, indicating the different influencing mechanisms of precipitation and evaporation in different soil layers (Table 1). These findings indicate that (1) the variations in the stable isotopes of soil water were primarily influenced by a combination of precipitation, infiltration, and evapotranspiration in the upper 40 cm of the soil profile, resulting in a less stable relationship between $\delta^{18}O$ and d-excess; (2) the variations may be predominantly caused by the migration of soil water from the top to the bottom via piston flow below a depth of 40 cm,; and (3) precipitation was an important source of soil water because negative

https://doi.org/10.5194/hess-2021-558
Preprint. Discussion started: 8 November 2021

Hydrology and Earth System Sciences
Open Access
EGU
Discussions

correlation between $\delta^{18}O$ and d-excess was significant in the study area.

Although all the soil layers exhibited a negative correlation between $\delta^{18}O$ and d-excess the correlation coefficients in the 40–60 cm and 80–100 cm soil layers were significant. This can be explained by three reasons as follows: (1) the 0–40 cm soil layer was more exposed to external disturbances, such as precipitation infiltration, evapotranspiration, and soil temperature; (2) observational studies have revealed that soil water is relatively low at a depth of approximately 60 cm in the soil profile, forming a significant "thinning and drying layer" (Li et al., 2010); and (3) the soil water movement was dominated by piston flow. A significant negative correlation was observed between $\delta^{18}O$ and d-excess on sunlit slopes, whereas the correlation was weaker for shady slopes. In addition, the slope was steeper and intercept was positive for the EL of shady slopes; however, the slope was less steep and intercept was negative for the EL of sunlit slopes, indicating high evapotranspiration due to long sunshine hours. For different vegetation types, the correlation between $\delta^{18}O$ and d-excess was ranked as forest > meadow > grassland, indicating the effect of vegetation conditions on the stable isotope values of soil water. This was also confirmed by the variations in slope and different intercepts for the ELs corresponding to the different vegetation types (Table 1).

3.2 Distribution of stable isotopes along soil profile

In the Three-River Headwater Region, $\delta^{18}O$ and $\delta^{2}H$ values first increased in the 0–40 cm soil layer, then decreased in the 40–80 cm soil layer, and increased again in the 80–100 cm soil layer (Fig. 4). The maximum values of $\delta^{18}O$ (-10.8‰) and $\delta^{2}H$ (-80.82‰) appeared in the 0–40 cm soil layer, and the minimum values ($\delta^{18}O$: -13.87‰; $\delta^{2}H$: -104.06‰) occurred in the 60–80 cm soil layer. The second highest isotope values were observed in the 80–100 cm soil layer. These results corresponded to the

https://doi.org/10.5194/hess-2021-558
Preprint. Discussion started: 8 November 2021

enrichment of δ^2H and $\delta^{18}O$ in the surface layer via evaporation, and evaporation decreased with increasing depth. The results also indicated the influence of soil water movement, whereby “new” water pushes “old” water down via piston flow, and soil water infiltrates along fast channels. Thus, the stable isotope content exhibited a bimodal pattern in the vertical soil profile due to priority flow, characterizing movable and immovable water. In unsaturated soil, piston flow was less pronounced at high soil water contents, whereas priority flow was more pronounced at low soil water contents. Piston flow and priority flow resulted in varying soil water distributions. Hence, these processes changed the distribution of stable isotopes in the study area and led to relatively positive stable isotope values at the bottom of the soil profile.

However, evaporation reduced the d-excess, as evidenced by the variations and maximum–minimum distribution of d-excess in the study area. Overall, the d-excess increased from 0 cm to 100 cm along the soil profile. The maximum d-excess value of 4.88‰ occurred in the 60–80 cm soil layer, whereas the minimum values of 3.95‰ and 3.91‰ appeared in the 0–20 cm and 20–40 cm soil layers, respectively; however, the d-excess value in the 80–100 cm soil layer was lower than that in the 60–80 cm soil layer. This was likely because the 0–40 cm soil layer was the major water supply layer for plants, and the effect of evapotranspiration was stronger in this layer than that in deeper soil layers. In contrast, soil water movement primarily affected the variations in the stable isotopes of soil water below a depth of 40 cm.

As shown in Fig. 4, same trend was observed for the variations in stable isotopes along the soil profiles in the source regions of the Yangtze and Yellow rivers. In the source region of the Lancangjiang River, the maximum isotope values ($\delta^{18}O$: -11.66‰; δ^2H: -81.76‰) appeared in the 80–100 cm soil layer, whereas the minimum values ($\delta^{18}O$: -15.89‰; δ^2H:

-121.56‰) occurred in the 0–20 cm soil layer. The second highest isotope values were observed in the 20–40 cm soil layer. These characteristics may be explained by two reasons: one is that precipitation infiltration caused the negative stable isotope values in the top soil layer, whereas the lower soil layer was influenced by soil water movement via piston flow and preferential flow. This understanding was confirmed by the variations in the d-excess values.

The same pattern was also observed in the regions with different vegetation types. For forested areas, the maximum $\delta^{18}O$ (-11.54‰) and $\delta^{2}H$ (-88.74‰) values appeared in the 20–40 cm soil layer, whereas the minimum values ($\delta^{18}O$: -15.75‰; $\delta^{2}H$: -113.38‰) occurred in the 60–80 cm soil layer. This was likely because the 20–40 cm soil layer was the major water supply layer for plants, and evapotranspiration was higher in this layer than in the 40–60 cm soil layer. The second highest isotope values were observed in the 80–100 cm soil layer under the influence of soil water movement.

On sunlit slopes, the $\delta^{18}O$ value first decreased from 0 cm to 80 cm and then increased in the 80–100 cm soil layer. The maximum $\delta^{18}O$ (-11.54‰) and $\delta^{2}H$ (-88.74‰) values appeared in the 0–20 cm soil layer, whereas the minimum values ($\delta^{18}O$: -14.26‰; $\delta^{2}H$: -104.86‰) occurred in the 60–80 cm soil layer. On shady slopes, the maximum $\delta^{18}O$ (-10.66‰) and $\delta^{2}H$ (-78.90‰) values appeared in the 20–40 cm soil layer, primarily due to water absorption by vegetation roots. These results corresponded to the enrichment of stable isotopes in the top soil layers under the influence of surface evaporation, and evaporation decreased with increasing soil depth.

3.3 Spatial distribution of stable isotopes

As shown in Fig. 5, the mean $\delta^{18}O$ value of soil water throughout the soil profile (0–100 cm) gradually became more positive from the southeast to

https://doi.org/10.5194/hess-2021-558
Preprint. Discussion started: 8 November 2021

the northwest in the source regions of the Yangtze and Yellow rivers, whereas it became more negative from the southeast to the northwest in the source region of the Lancangjiang River. Interestingly, no evident variation trend was observed for the stable isotope values throughout the soil profile (0–100 cm), which also indicated the complexity and diversity of the influencing factors, such as evaporation, soil water movement, vegetation growth, and soil water sources, on soil water.

The $\delta^{18}O$ values in the 0–20 cm soil layer were nearly positive, particularly in the northern and southern regions. However, there was a decreasing trend toward the central and eastern parts, which was likely due to low evaporation and the mixing effects of new precipitation at relatively higher altitudes. Notably, the same pattern was not observed between the $\delta^{18}O$ values of surface soil water (0–20 cm) and precipitation; however, this did not include the source region of the Lancangjiang River, where the $\delta^{18}O$ value of soil water decreased with increasing precipitation from lower to higher altitudes. The influence of evaporation on the isotopic composition of the surface soil water was considerably greater than that on the isotopic composition of any other soil layer, and the higher the evaporation, the more enriched the $\delta^{18}O$ content.

Overall, the $\delta^{18}O$ value in the 20–40 cm soil layer exhibited a decreasing trend from the southeastern part to northwestern part of the study area. The low values were primarily distributed in the Tanggula Mountains, source region of the Lancangjiang River, Bayankara Mountains, and Animaqing Mountains, whereas the high values were primarily distributed in the Kunlun, Ruoerge, and outflow areas of the source region of the Yellow River. The influence of evaporation on the isotopic composition decreased with increasing soil depth, and the influence of precipitation, temperature, topography, and other factors were more prominent in the deeper soil layers. In addition, because the

https://doi.org/10.5194/hess-2021-558
Preprint. Discussion started: 8 November 2021

upper soil layer was the major water source for plants, particularly in meadows, this layer had relatively positive $\delta^{18}O$ values under the influence of water uptake and evapotranspiration by the vegetation root system.

Negative $\delta^{18}O$ values were primarily distributed in the 40–60 cm soil layer in the Zhaqu River basin, Tuotuohe River basin, and Bayankara Mountains. However, the $\delta^{18}O$ value was mostly depleted in the Kunlun Mountains, Tongtianhe River basin, and most parts of the source region of the Yellow River, which was co-influenced by plant water use, soil water sources, and soil water movement.

The area with negative $\delta^{18}O$ values in the 60–80 cm soil layer increased significantly compared with that in the 40–60 cm layer, particularly in the Tuotuohe River basin, Zhaqu River basin, and Ruoergai region. However, mostly positive $\delta^{18}O$ values were observed in the source region of the Lancangjiang River, central source region of the Yangtze River, and northern fringe of the Yellow River source region. This change was primarily caused by soil water movement, which affected the variations in stable isotopes in the soil profile.

In the bottom soil layer (80–100 cm), the $\delta^{18}O$ value gradually became more positive from the southern part toward the northern part of the study area. This trend was identical with the latitudinal effect of stable isotopes in precipitation, indicating that precipitation was the major source of soil water recharge in the active permafrost layer.

The d-excess value throughout the soil profile (0–100 cm) gradually increased from the southern part to the northern part of the study area, which was the opposite distribution to that observed for $\delta^{18}O$ (Fig. 6). In the 0–20 cm soil layer, the mean d-excess value was relatively low (5.18‰), widely ranging from -11.24‰ to 21.39‰. Throughout the study area, the d-excess value was higher in the north than in other areas and

https://doi.org/10.5194/hess-2021-558
Preprint. Discussion started: 8 November 2021

was the lowest in the southeast. High d-excess values were primarily distributed in the Kunlun Mountains, Tanggula Mountains, Bayan Kara Mountains, and Animapro Mountains. The relatively low d-excess values were primarily observed in the source region of the Lancangjiang River and the marginal and headwater areas of the Yellow River, which was due to the relatively low evaporation at high latitudes.

In the 20–40 cm soil layer, the mean d-excess value was 5.13‰, ranging from -13.35‰ to 22.30‰. The high values were observed in the source regions of the Yangtze River and Lancangjiang River, particularly in the Tanggula and Kunlun mountains; however, lower values were primarily distributed in the source region of the Yellow River, particularly in the headwater area.

In the 40–60 cm soil layer, the d-excess value ranged from -13.35‰ to 22.30‰, with a mean of 5.71‰. The lower values were primarily observed in the low altitude areas of the Yangtze and Yellow rivers and the Bayan Kara Mountains, whereas the higher values were primarily distributed in the Tanggula and Kunlun mountains.

In the 60–80 cm soil layer, the d-excess value ranged from -8.94‰ to 18.36‰, with a mean of 5.85‰. Spatially, the value varied considerably in this soil layer, increasing from the south to the north in the source region of the Yangtze and Yellow rivers but from north to south in the source region of the Lancangjiang River. The high d-excess values were primarily distributed in the Kunlun Mountains, Bayan Kara Mountains, and the central source region of the Yellow River.

Among all soil layers, the highest mean d-excess value (6.11‰, ranging from -8.30‰ to 16.66‰) was observed in the 80–100 cm soil layer. Relatively high values were distributed in the Kunlun Mountains, central area of the Yellow River, and source region of the Lancangjiang River. Overall, with increasing soil depth, the d-excess value increased,

https://doi.org/10.5194/hess-2021-558
Preprint. Discussion started: 8 November 2021

and the variation range became smaller and more positive.

3.4 Soil evaporation based on stable isotopes

The variations in the lc-excess are shown in Fig. 7. The mean values of $\delta^{18}O$, $\delta^{2}H$, and lc-excess for precipitation in the study area were -14.25‰, -100.84‰, and -0.83‰, respectively, whereas those for soil water were -12.05‰, -90.76‰, and -8.10‰, respectively. These differences indicate that the isotopic enrichment of soil through evaporation occurred with precipitation infiltration to the soil. Moreover, there were high variations in stable isotopic compositions.

Temporally, the maximum lc-excess of precipitation occurred in April, whereas the minimum was in February. Moreover, the lc-excess in soil water was significantly influenced by precipitation infiltration. The lc-excess values of soil water in the 0–20 cm, 20–40 cm, 40–60 cm, 60–80 cm, and 80–100 cm soil layers were -8.48‰, -8.51‰, -8.12‰, -7.88‰, and -7.54‰, respectively. Hence, the lc-excess value increased gradually with increasing soil depth, and the degree of variation decreased. Similar patterns were observed in the source regions of the Yangtze River, Yellow River, Lancangjiang River, and the entire study area. The minimum lc-excess value occurred in the 80–100 cm soil layer in the source region of the Yangtze River, whereas the maximum lc-excess value occurred in the 80–100 cm layer in the source region of the Lancangjiang River. The mean lc-excess values were -7.55‰, -7.65‰, and -7.93‰ in the source regions of the Yangtze River, Yellow River, and Lancangjiang River, respectively. These results indicated how the stable isotopes of surface soil water are influenced by evaporation and precipitation infiltration during the rainy season, whereas they are primarily influenced by soil water movement in the deeper layers. Moreover, the degree of influence also varied significantly owing to the differences in climatic conditions, geomorphology, and vegetation types in the source regions.

The mean lc-excess values for grasslands, meadows, and forest were -8.62‰, -5.92‰, and -7.24‰, respectively, which primarily reflected the differences in evaporation effects. In addition, the lc-excess values exhibited an increasing trend from 0 cm to 100 cm but with varying degrees. For grassland areas, the maximum and minimum values appeared in the 20–40 cm and 40–60 cm soil layers, respectively, and the values in the other soil layers were similar. For meadow areas, the maximum and minimum values occurred in the 40–60 cm and 20–40 cm soil layers, respectively, and the values in the other soil layers were similar. For forest areas, the maximum and minimum appeared in the 60–80 cm and 0–20 cm soil layers, respectively, and other soil layers exhibited variations. These features indicated the following influences of vegetation on the stable isotope profiles of soil water. (1) The isotopes of surface soil water were primarily influenced by evaporation and precipitation infiltration with substantial variations; (2) the major water absorption layers for grassland, meadow, and scrub roots were probably the 20–40 cm, 40–60 cm, and 60–80 cm soil layers, respectively, which were influenced by vegetation transpiration and had relatively positive stable isotopes; and (3) the most intense evapotranspiration was observed in the meadow area with good vegetation conditions. Figure 7 shows that the lc-excess values were significantly higher on sunlit slopes than on shady slopes, confirming the intense evapotranspiration. In addition, the variation pattern of lc-excess with soil profile depth differed between shady and sunlit slopes, indicating the complex mechanism of stable isotopes in soil water.

3.5 Relationship between soil water and surface waters

In the study region, the LMWL was $\delta^2H = 7.89\delta^{18}O + 12.43$ ($R^2 = 0.97$; $N = 375$) based on event-level precipitation. Figure 8 shows that

https://doi.org/10.5194/hess-2021-558
Preprint. Discussion started: 8 November 2021

soil water was primarily located on the LWML, suggesting that precipitation was the major soil water source, and some soil water plotted below the LWML indicated high evaporation. Moreover, the main stream water and tributary water clustered between supra-permafrost water and soil water, indicating a hydraulic relationship between recharge and discharge. This suggests that water from the sources first infiltrated forming soil water, which then transformed to recharge the supra-permafrost water. This supra-permafrost water subsequently recharged the tributary or main stream water, indicating the uniqueness of the runoff-initiating and converging processes in cold regions and confirming the significant influence of permafrost on the hydrological process. This interpretation suggests that precipitation did not directly replenish surface runoff in the study area. This could be due to the transformation of precipitation into soil water or supra-permafrost water that is stored in the permafrost active layer, which has a significant influence on the runoff process. Similar results were also reported for the Qilian Mountains (Li et al., 2019), likely indicating the unique hydrological processes, particularly in glaciers and permafrost regions. Overall, the isotopic compositions of soil water were close to the LMWL, and the $\delta^{18}O$ and $\delta^{2}H$ values varied between precipitation and ground ice. Accordingly, it can be inferred that soil water in the study area is recharged by multiple sources.

The relationship between soil water and the LWML varied significantly at different altitudes; the lower the altitude, the lower the left-hand side of the LWML, and vice versa. The slope and intercept of the EL also confirmed this relationship, whereby the lowest slope and intercept values occurred at 3000–3500 m, which increased with increasing altitude to maximum vales at 3500–4000 m and 4500–5000 m, respectively. These results confirmed that the degree of influence of

https://doi.org/10.5194/hess-2021-558
Preprint. Discussion started: 8 November 2021

evapotranspiration on stable isotopes decreased with increasing altitude. The stable isotope values of soil water were generally clustered and distributed with precipitation at different altitudes, indicating that precipitation was the major soil water source in the study area.

The relationship between soil water and the LWML also varied significantly with vegetation types, with forest being farthest from the LWML, followed by meadows and grasslands. The slope and intercept of the EL for each vegetation type also confirmed this trend (Fig. 8). Owing to the high water consumption and evapotranspiration, the stable isotope values of soil water were relatively positive in the forest areas. The meadow region had a lush vegetation growth condition and high evapotranspiration. Moreover, the soil was unconsolidated with capillary development, which likely had a relatively strong influence on stable isotopes. In addition, the relationship between soil water and the LWML varied significantly between shady and sunlit slopes. Soil water was far from the LWML on sunlit slopes, whereas it was closer to the LWML on shady slopes under the influence of evapotranspiration. These variations also indicated the difference in the recharge ratio between precipitation and ground ice to soil water at different elevations, vegetation, and slope directions.

3.6 Sources of soil water

The EMMA model was used to identify different source areas and the mixing processes of soil water and quantify the contribution of each endmember. There were significant differences in the δ^2H and $\delta^{18}O$ concentrations of ground ice, precipitation, and soil water in the study area (Fig. 8). Accordingly, these $\delta^{18}O$ and δ^2H data were selected for analysis because they could effectively characterize the sources. There were large spatiotemporal variations in the $\delta^{18}O$ and δ^2H concentrations and soil water plotted on a straight line spanning the two endmembers, suggesting that soil water was a mixture of them (Fig. 9). Therefore, precipitation was considered as the first endmember and ground ice as the second endmember. Soil water was also characterized during the sampling period (Fig. 9). In the study region, precipitation and ground ice accounted for approximately 88% and 12% of soil water, respectively, in July 2019; hence, precipitation was the major source of soil water in July, which is the rainy season. However, a large amount of ground ice likely melted before July as soil temperatures increased, particularly in shallow soils.

On sunlit slopes, the estimated contributions of precipitation and ground ice to soil water were approximately 90% and 10%, respectively, whereas those on shady slopes were approximately 86% and 14%, respectively (Fig. 10). This difference can be explained by the following reasons. (1) The effect of solar radiation was stronger on sunlit slopes, as the soil temperature was higher, ground ice melted faster, and melting period started earlier than on shaded slopes; hence, the ground ice content was higher on shady slopes. (2) Evapotranspiration was higher on sunlit slopes than on shady slopes, whereas the soil water content was lower on sunlit slopes than on shady slopes. In addition, piston flow development was more favorable on sunlit slopes when precipitation occurred, as the soil acted as a “dry sponge” with a strong capacity to absorb water.

The soil water sources also varied significantly at different elevations (Fig. 10). The area below 3700 m was characterized by seasonally frozen soil, where the major soil water source was precipitation because the seasonally frozen soil melted before July; therefore, ground ice did not contribute to soil water in this region. For the area above 3700 m, the contribution of precipitation to soil water gradually decreased with increasing altitude, whereas the contribution of ground ice gradually increased but fluctuated. A higher contribution of precipitation was observed in the zones of 3900–4100 m, 4300–4500 m, and 4700–4900 m, whereas ground ice contributed more to soil water in the zones of 4500–4700 m and 4900–5100 m. Thus, as temperature increased with a decrease in elevation, the earlier the ground ice melted, the greater the melting intensity. In addition, the distribution of ground ice was uneven owing to various factors, such as topography, geology, and groundwater.

The soil water sources also varied significantly with different vegetation zones (Fig. 10). The forest area is primarily located in the region of seasonally frozen soil, where soil water is primarily recharged by precipitation. Precipitation contributed approximately 84% and 80% to soil water in grassland and meadow areas, respectively, , whereas ground ice contributed approximately 16% and 20%, respectively. The soil water content was high in the meadow area because of the lush vegetation growth. The supra-permafrost water level was also high, and the ground ice storage was abundant and mostly distributed on shady or semi-shady slopes. Furthermore, a previous study reported that ground ice was abundant during July in meadows with high vegetation cover than in grasslands (Li et al., 2010). Interestingly, with the increase in soil profile depth, the contribution of precipitation to soil water gradually decreased, whereas the contribution of ground ice gradually increased (Fig. 10). The reasons for this are as follows: i) ground ice storage increases with increasing soil profile depth, ii) ground ice melts earlier on the surface, and iii) precipitation primarily recharges soil water through piston flow.

4. Discussion

4.1 Influence of altitude on stable isotopes

Stable isotopes of soil water are influenced by multiple factors such as precipitation, evaporation, soil water movement, vegetation type, topography, and human activities (Matthias et al., 2017). Although stable

https://doi.org/10.5194/hess-2021-558
Preprint. Discussion started: 8 November 2021

isotopes of soil water were affected by altitude (Fig. 11), no evident effect was observed for the 0–20 cm soil layer, likely due to intense solar radiation and evaporation from the surface soil. Moreover, precipitation infiltration occurred primarily at the surface, leading to random variations in stable isotopes and an irregular trend with increasing elevation. The rate of change in $\delta^{18}O$ with increasing altitude was -0.11‰/100 m (R^2 = 0.013), 0.37‰/100 m (R^2 = 0.08), 0.02‰/100 m (R^2 = 0.12), and 0.02‰/100 m (R^2 = 0.02), at soil depths of 20–40 cm, 40–60 cm, 60–80 cm, and 80–100 cm, respectively. Hence, altitude evidently affected the $\delta^{18}O$ values of soil water in the 20–60 cm soil layer, whereas it was less pronounced in the 60–100 cm soil layer. The $\delta^{18}O$ value increased with increasing altitude throughout 40–100 cm soil layer. These changes indicate that precipitation infiltration was not the major factor affecting the variations in soil water in the 20–100 cm soil layer with increasing altitude. Alternatively, soil hydrological processes and other factors played significant roles. With increasing altitude, the d-excess value increased in the 0–40 cm soil layer and then decreased in the 40–100 cm soil layer. The rate of change in d-excess with increasing altitude was 0.43‰/100 m (R^2 = 0.09), 0.13‰/100 m (R^2 = 0.005), -0.64‰/100 m (R^2 = 0.02), -0.54‰/100 m (R^2 = -0.02), and -0.69‰/100 m (R^2 = -0.02) in the 0–20 cm, 20–40 cm, 40–60 cm, 60–80 cm, and 80–100 cm soil layers, respectively.

For grassland, the rate of change in $\delta^{18}O$ with increasing altitude was -0.22‰/100 m (R^2 = -0.02), -0.106‰/100 m (R^2 = -0.002), 0.34‰/100 m (R^2 = 0.02), 0.46‰/100 m (R^2 = -0.02), and -0.125‰/100 m (R^2 = -0.083) in the 0–20 cm, 20–40 cm, 40–60 cm, 60–80 cm, and 80–100 cm soil layers, respectively. The rate of change in d-excess value with increasing altitude was 0.54‰/100 m (R^2 = 0.15), 0.15‰/100 m (R^2 = -0.01), -0.45‰/100 m (R^2 = -0.01), 0.16‰/100 m (R^2 = -0.07), and -0.43‰/100 m (R^2 = -0.083) in the 0–20 cm, 20–40 cm, 40–60 cm, 60–80 cm, and 80–100 cm soil layers, respectively. These gradients confirm that the soil layer above 40 cm in the grassland area was primarily influenced by evapotranspiration, whereas the influence of other factors (such as soil water movement) dominated below 40 cm.

In the meadow area, except for the 20–40 cm soil layer (-0.15‰/100 m; R^2 = -0.06), there was no significant altitude effect on the $\delta^{18}O$ values of other soil layers. However, the rate of change in d-excess with increasing altitude was -0.14‰/100 m (R^2 = -0.03), 0.23‰/100 m (R^2 = -0.02), -0.18‰/100 m (R^2 = -0.05), 0.25‰/100 m (R^2 = -0.17), and -1.5‰/100 m (R^2 = 0.55) in the 0–20 cm, 20–40 cm, 40–60 cm, 60–80 cm, and 80–100 cm soil layers, respectively. These gradients indicate that the altitude effect was not significant in the meadow area owing to strong evaporation, high soil water content, freeze–thaw processes, and soil water movement.

In addition, the altitude effect was slightly more pronounced on sunlit slopes than on shady slopes, which also indicated the complex coupling process between moisture–soil–vegetation and freeze–thaw processes in the permafrost region. Therefore, continuous observations and sampling are key to studying ecohydrological processes in cold regions.

Therefore, unlike the stable isotopes of precipitation and river water, the stable isotopes of soil water did not vary significantly with altitude. This can be explained by three possible reasons. (1) Soil water flows downhill along the slope under gravity due to lateral recharge at higher altitudes, implying that soil water may be insufficient and variable. Thus, soil water at high altitudes is characterized by low soil water dynamics with positive stable isotope values under the influence of evapotranspiration. (2) A relatively flat topography effectively reduces the lateral movement of soil water at low altitudes. Flat areas at low altitudes can also receive soil water from high altitudes and be recharged by rivers or upward infiltration from supra-permafrost water, resulting in sufficient soil water with negative stable isotopes. (3) Furthermore, vegetation cover is sparse at high altitudes, leading to relatively weak water-holding capacity. However, the high vegetation coverage at low altitudes promotes long-term accumulation of soil water, high soil water content, and negative stable isotopes.

4.2 Influences of soil temperature and moisture on stable isotopes

Soil temperature and moisture not only affect regional runoff production, infiltration, evapotranspiration, and vegetation evolution, but also the distribution of energy and thermal parameters (Carey and Feng, 2004). Hu et al. (2014) revealed that a decline in soil temperature caused soil water to migrate to the upper and lower freezing fronts during the freezing period, whereas the middle part of the active layer was evacuated and dried. As shown in Fig. 12, with increasing soil moisture, the $\delta^{18}O$ value decreased ($\delta^{18}O$ = -0.046H - 9.93; R^2 = 0.024), whereas the d-excess value increased (d-excess = 0.18H - 0.27; R^2 = 0.09) throughout the study area. Thus, the higher the soil moisture content, the more negative the stable isotope value, and vice versa. This corresponds well with the variation pattern between the stable isotopes of precipitation and air humidity. These results confirm that precipitation was the major soil water source in this study and that high soil water content may have resulted in a low evaporation effect on stable isotopes with increasing soil depth. The relationship between $\delta^{18}O$ and soil moisture was also inconsistent for each soil layer. The negative correlation between $\delta^{18}O$ and soil moisture decreased with increasing soil depth and became positive below a depth of 60 cm. However, d-excess and soil moisture were positively correlated in all soil layers except the 20–40 cm soil layer,

https://doi.org/10.5194/hess-2021-558
Preprint. Discussion started: 8 November 2021

and the correlation coefficient gradually increased with increasing soil depth, reaching the maximum in the 80–100 cm soil layer (Table 2). These findings indicate that (1) the stable isotopes of surface soil water were significantly influenced by frequent precipitation infiltration during the rainy period; (2) the 20–60 cm soil layer provided the major moisture source for grassland with relatively high evapotranspiration, and the soil water was replenished by ground ice, which weakened the relationship between stable isotopes and soil water; and (3) the stable isotopes below the 60 cm soil layer were primarily affected by soil water movement and ground ice.

For different vegetation types, the correlation between stable isotopes and soil moisture was most significant in the forest area, followed by the grassland area; however, it was relatively weak in the meadow area. Forests primarily depend on deep soil water or groundwater, and evaporation is relatively weak under the shade of trees; therefore, soil water can retain information regarding precipitation. The meadow area had the higher levels of soil moisture and vegetation growth than the grassland area. Moreover, the meadow area had a “grass carpet layer,” which was rich in vegetation, and had a well-developed root system; thus, precipitation could quickly infiltrate the deep soil, with a small part being absorbed and retained by the root system, leading to no flow in the shallow soil. However, deeper soil water could be mixed by precipitation infiltration, thereby affecting the stable isotope content. In addition, the correlation between stable isotopes and soil moisture was relatively weaker on sunlit slopes than on shady slopes.

As shown in Fig. 12, soil temperature exhibited a weak positive correlation with $\delta^{18}O$, whereas it exhibited a negative correlation with d-excess. Thus, it was confirmed that the higher the soil temperature, the more intense the evapotranspiration, resulting in a more positive stable

https://doi.org/10.5194/hess-2021-558
Preprint. Discussion started: 8 November 2021

isotope value. However, the relationship between $\delta^{18}O$ and soil temperature varied significantly between soil layers, exhibiting a weak positive correlation for the 20–60 cm soil layer but a negative correlation for the 0–20 cm and 60–100 cm soil layers (Table 3). This can be explained by three main reasons. (1) Surface soil water is jointly affected by precipitation infiltration and evapotranspiration, resulting in large variations in $\delta^{18}O$. (2) The $\delta^{18}O$ value of soil water in the 20–60 cm layer was primarily affected by vegetation evapotranspiration. (3) The 60–100 cm soil layer was primarily dominated by soil water movement. Overall, the d-excess of soil water exhibited a significant positive correlation with the soil temperature.

The mean soil temperature of different vegetation types decreased in the order of forest > grassland > meadow. Except for grassland, the $\delta^{18}O$ values of soil water in the meadow and forest areas were positively correlated with soil temperature. In contrast, d-excess was significantly negatively correlated with soil temperature, and the correlation level was consistent with the variation in soil temperature. In addition, the correlation coefficients between stable isotopes and soil temperature were significantly high on sunlit slopes than on shady slopes. These findings indicate that soil temperature is an important indicator of the degree of influence of evapotranspiration on stable isotopes and that this influence varies with soil depth, vegetation type, and slope direction.

4.3 Influence of vegetation conditions on stable isotopes

Figure 13 shows that the mean values of $\delta^{18}O$ and d-excess were -11.32‰ (ranging from -20.86‰ to -0.74‰) and 5‰ (ranging from -15.46‰ to 22.30‰), respectively, in the grassland area, -11.63‰ (-19.26‰ to -5.68‰) and 7.87‰ (-5.07‰ to 24.46‰), respectively, in the meadow area, and -12.89‰ (-16.09‰ to -9.47‰) and 7.87‰ (-4.73‰ to 17.48‰), respectively, in the forest area. Interestingly, the slope and intercept of EL

https://doi.org/10.5194/hess-2021-558
Preprint. Discussion started: 8 November 2021

increased in the order of forest, meadow, and grassland. This indicates that the vegetation type is closely related to the variations in the stable isotopes of soil water. To further analyze the effect of vegetation conditions on the stable isotopes of soil water, the relationship between vegetation cover, vegetation height, and root depth and stable isotopes were analyzed as follows.

Vegetation cover was negatively correlated with $\delta^{18}O$ and d-excess (Fig. 13). Generally, the higher the vegetation cover and the stronger the evapotranspiration, the more positive the $\delta^{18}O$ value and the more negative the d-excess value. For specific layers, the $\delta^{18}O$ value in the 0–60 cm soil layer was significantly negatively correlated with vegetation cover; however, a positive correlation was observed in the 60–100 cm soil layer, where d-excess was negatively correlated with vegetation cover. These results indicate that precipitation infiltration had some influence on soil water with a higher vegetation cover due to root pore space and soil looseness, whereby soil water could be gradually replenished after being removed by evapotranspiration. Moreover, the variations in the stable isotopes of soil water were primarily influenced by evapotranspiration in areas with relatively low vegetation cover. For the soil layer below 60 cm, the influence of vegetation cover continued to weaken, and the variations in stable isotopes were relatively stable. Zimmermann et al. (1966) also reported that stable isotope profiles were enriched in bare soil conditions compared with grass-covered areas.

The grass height was positively correlated with the $\delta^{18}O$ value of soil water, whereas d-excess was negatively correlated both throughout the soil profile and in each soil layer. The higher the grass height, the greater the evapotranspiration effect, the more positive the $\delta^{18}O$ value, and the more negative the d-excess value. Therefore, grass height can be an indicator of the degree of vegetation evapotranspiration. Vegetation root

https://doi.org/10.5194/hess-2021-558
Preprint. Discussion started: 8 November 2021

depth exhibited a weakly negative correlation with $\delta^{18}O$, whereas it exhibited a non-significant positive correlation with d-excess. In terms of specific soil layers, $\delta^{18}O$ was positively correlated and d-excess was negatively correlated with root depth in the 0–20 cm and 80–100 cm layers; however, the reverse was true for the 20–80 cm soil layer. Accordingly, it can be inferred that (1) the effect of high evapotranspiration is primarily concentrated in the surface soil, whereas soil water movement is more complex and influenced by multiple factors; (2) rapid precipitation infiltration is more favorable with increased root system, thereby mixing soil water and leading to more negative stable isotope values; (3) vegetation primarily absorbs deep soil water, and the deeper the root system, the less effective the evapotranspiration. Wang et al. (2010) also confirmed that plant roots have no fractionation effect on stable isotopes in soil water because they remove both heavy and light isotopes from soil water, resulting in a slow development of the isotope profile.

4.4 Soil water: Sources and implications for ecological protection

This study confirmed that precipitation is the major soil water source in the permafrost active layer and that the degree of influence of precipitation on soil water varies significantly depending on the topography, vegetation, soil texture, and freeze–thaw processes. Wu et al. (2021) revealed that both soil water and daily mean precipitation exhibited the same spatial pattern on the Qinghai–Tibet Plateau, whereas the northwestern arid region had low precipitation and low soil water. Evapotranspiration is the major process through which soil water dissipates in the permafrost active layer. On the one hand, evapotranspiration causes the variations in the soil water content, which in turn changes the stable isotope profiles. On the other hand, evapotranspiration also influences the changes in vegetation and freeze–

thaw processes, ultimately causing spatiotemporal changes in soil water. In addition, evapotranspiration varies significantly with vegetation type and soil type, thereby resulting in significant differences in stable isotope profiles.

Physical and chemical properties of soil are the key determinants of soil water movement, and environmental factors affecting soil water infiltration primarily include bulk density, porosity, soil texture, organic matter content, and the number of particles with diameter of < 0.1 mm (Zhu et al., 2017). Moreover, soil represents a precondition that determines the occurrence of preferential flow or piston flow in soil, which profoundly influences the changes in the soil water profile. When the active layer is in a frozen state, the unfrozen water exhibits an overall upward trend under the effect of temperature gradients. After the active layer has completely thawed, precipitation moves under the influence of gravity, and the amount of water migration is thus higher (Jiao et al., 2014). The distribution and volume of ground ice in permafrost differ spatially owing to regional variations in climate, topography, ecosystems, and permafrost development (Kanevskiy et al., 2014); thus, the impact of ground ice on soil water is also stochastic. Moreover, the near-surface ground ice content has been closely correlated with surface soil and vegetation parameters, with the strongest correlations observed for locations with the longest landscape-development time (Wang et al., 2019; Fan et al., 2021).

Vegetation differences also have a significant effect on soil water. Li et al. (2020) reported that the aboveground and belowground biomasses in alpine meadows were 2 and 2.5 times higher than those in alpine grasslands. In addition, the root system of alpine meadows was primarily dense, with a stronger water-holding capacity and water-blocking function than that of alpine grasslands. The dry surface soil of alpine meadows first recharges when precipitation occurs, thereby reducing the recharge of deep soil water below a depth of 20 cm. During the complete soil thaw in summer, there was one low water-bearing layer (~50 cm) and two relatively high water-bearing layers (20 cm and 120 cm) in the active layer of alpine meadows; however, there was a consistent increasing tendency for soil water with increasing depth in alpine grasslands (Liu et al., 2009). Jiao et al. (2014) revealed that the onset of soil freezing in alpine meadows lagged than in alpine grassland by 3–15 d during the autumn freezing period. Moreover, Niu et al. (2019) reported that the soil water content was higher in regions with higher vegetation cover. With decreasing vegetation cover, Liu et al. (2009) observed that the rate of variation of soil temperature and water content increased, and the onset dates of ground surface thawing and freezing advanced.

Permafrost, as an impermeable layer, prevents soil water from infiltrating downward. During thawing, the downward hydrothermal process becomes more active because of the increase in short-wave radiation from the ground. Thus, the thawed water is quickly absorbed by the soil, and the deep soil water migrates to the shallow soil (Yang et al., 2013; Wu et al., 2018). Permafrost degradation leads to the changes in the microstructure, porosity, and infiltration properties of soil at the micro level, thereby affecting the changes in the microstructure and seepage characteristics of the permafrost layer, ultimately causing soil water movement and changes in it (Schuur and Mack, 2018). In addition, seasonal freeze–thaw processes affect soil water migration toward the freezing front in the soil profile (Fu et al., 2018). Under a warming climate, a delayed onset of ground freezing and faster thaw completion would result in reduced availability of near-surface soil water in spring (Yang and Wang, 2019).

In areas with a high active layer thickness and a low ground ice content, permafrost degradation leads to increased soil water infiltration and limited soil water recharge from the frozen storage of previous year, thereby reducing soil water and causing vegetation degradation. Moreover, the recharging water above the permafrost layer is sharply reduced with decreasing soil water, and the low marsh wetlands shrink significantly. These changes lead to the succession of alpine marshy meadows to alpine meadows and alpine grasslands, with consequent changes in vegetation cover and root systems. These changes weaken influence of vegetation on soil water and reduce the ability of the system to hold and transport surface water, resulting in serious water loss.

Therefore, establishing an observation network and monitoring permafrost degradation in the Three-River Headwater Region are critical . In particular, conducting systematic research on soil water changes in the active permafrost layer and exploring the impact of permafrost degradation on soil water variation and vegetation growth are necessary. Furthermore, there is an urgent need to develop technologies for fragile ecosystem restoration and improve the water conservation capacity for wetland ecosystem restoration/conservation, soil and water conservation enhancement, and ecological adaptation and regulation of climate change. Based on the above-mentioned aspects, it is necessary to vigorously implement ecological protection and construction projects, natural forest protection projects, and the conversion of cropland to forest and grassland projects. Such strategies could effectively deal with ecological problems, such as decreased water conservation capacity, increased soil erosion, and vegetation degradation, caused by future permafrost degradation.

5. Conclusions

The permafrost active layer plays an important role in ground–air exchange, surface processes, and the hydrological cycle. Based on the study of 1140 samples of soil water, precipitation, river water, ground ice,

https://doi.org/10.5194/hess-2021-558
Preprint. Discussion started: 8 November 2021

supra-permafrost water, and glacier snow meltwater, the soil water sources were quantified in the Three-River Headwater Region, which is currently experiencing widespread permafrost degradation. The results showed that the mean $\delta^{18}O$ and d-excess values of soil water were -11.58‰ and 5.77‰, respectively, and that there existed a negative correlation between them. The EL in the study region was $\delta^2H = 7.46\ \delta^{18}O - 0.37$. In the soil profile, the $\delta^{18}O$ and δ^2H values first increased, then decreased in the 0–80 cm soil layer, and increased again in the 80–100 cm soil layer. The mean $\delta^{18}O$ value became more positive gradually from the southeast to the northwest in the source regions of the Yangtze and Yellow rivers, whereas it became more negative from the southeast to the northwest in the source region of the Lancangjiang River. The variations in lc-excess values indicated that soil isotopic enrichment through evaporation occurred with precipitation infiltration to the soil. The stable isotopes of soil water did not exhibit significant altitude effects owing to i) the downslope flow of soil, ii) flat topography at lower altitudes, and iii) gradual increase in vegetation cover with decreasing altitude. The higher the soil water content, the more negative the stable isotope values, and vice versa. The higher the soil temperature, the more positive the stable isotope values of soil water. Vegetation cover was negatively correlated with both $\delta^{18}O$ and d-excess, whereas grass height was positively correlated with $\delta^{18}O$ and negatively correlated with d-excess. The stable isotopes of surface soil water were significantly influenced by the frequent infiltration of precipitation and evapotranspiration. The 20–60 cm soil layer was the major vegetation moisture source layer, which was primarily influenced by evapotranspiration and ground ice. The stable isotopes below the 60 cm soil layer were primarily affected by soil water movement and ground ice mixing; however, they were weakly affected by evapotranspiration.

https://doi.org/10.5194/hess-2021-558
Preprint. Discussion started: 8 November 2021

Hydrology and Earth System Sciences
Open Access
EGU
Discussions

Based on stable isotope tracing, soil water was found to be primarily recharged by precipitation and ground ice in the study area. Precipitation and ground ice accounted for approximately 88% and 12% of soil water, respectively. The contribution of precipitation to soil water on sunlit slopes and shady slopes was approximately 90% and 86%, respectively. Higher precipitation contributions to soil water were observed in the 3900–4100 m, 4300–4500 m, and 4700–4900 m zones, whereas ground ice contributed more to soil water in the 4500–4700 m and 4900–5100 m zones. Precipitation contributed approximately 84% and 80% to soil water in grasslands and meadows, respectively, whereas ground ice contributed approximately 16% and 20%, respectively. Precipitation; evapotranspiration; physical and chemical properties of soil; and the distributions of ground ice, vegetation, and permafrost degradation were the major factors influencing the soil water sources in the permafrost active layer of the study area. Therefore, it is critical to establish an observational network, develop technologies for ecosystem restoration and conservation, and implement ecological protection and construction projects in the Three-River Headwater Region to effectively deal with ecological problems caused by future permafrost degradation.

Acknowledges

This study was supported by National Nature Science Foundation of and China(42077187), the Second Tibetan Plateau Scientific Expedition and Research Program (STEP, Grant No. 2019QZKK0405), the National Key Research and Development Program of China (Grant No. 2020YFA0607700), the "Western Light"-Key Laboratory Cooperative Research Cross-Team Project of Chinese Academy of Sciences, National "Plan of Ten Thousand People" Youth Top Talent Project, Innovative

https://doi.org/10.5194/hess-2021-558
Preprint. Discussion started: 8 November 2021

Hydrology and Earth System Sciences Discussions

Groups in Gansu Province (2020), Key Groups of Gansu Province (2020). We greatly appreciate suggestions from anonymous referees for the improvement of our paper. Thanks also to the editorial staff.

Author contributions

Zongxing Li designed research; Zongxing Li, Gui Juan performed research; Zongxing Li, Gui Juan, Baijuan Zhang, Feng Qi analyzed data; Zongxing Li and Gui Juan wrote the paper.

Competing interests

This manuscript has not been published or presented elsewhere in part or in entirety and is not under consideration by another journal. We have read and understood your journal's policies, and we believe that neither the manuscript nor the study violates any of these. There are no conflicts of interest to declare.

References

Brooks, P. D., J. Chorover, Y. Fan, S. E. Godsey, R. M. Maxwell, J. P. McNamara, &Christina Tague, 2015. Hydrological partitioning in the critical zone: Recent advances and opportunities for developing transferrable understanding of water cycle dynamics. Water Resources Research 51(9), 6973–6987. https://doi.org/10.1002/2015WR017039.

Cao W，Sheng Y，Wu J C，&Peng E X， 2021. Soil water infiltration characteristics of different types of frozen soil in the Source Area of the Yellow River . Acta Ecologica Sinica 41(2) , 655-664. https://doi.org/10.5846/stxb201903150491.

Carey Gazisa, &Xiahong Feng, 2004. A stable isotope study of soil water: evidence for mixing and preferential flow paths. Geoderma 119(1) 97–

111.https://doi.org/10.1016/S0016-7061(03)00243-X.

Carey Gazisa, &Xiahong Feng, 2004. A stable isotope study of soil water: evidence for mixing and preferential flow paths. Geoderma 119(1/2), 97–111. https://doi.org/10.1016/S0016-7061(03)00243-X.

Chang Juan, Wang Genxu, Gao Yongheng, &Wang Yibo, 2012. Influence of snow cover in permafrost region of Qinghai-Tibet Plateau on thermal process of soil water in shallow layer of swamp and meadow. Acta Ecologic Sinica 32 (23), 7289-7301. https://doi.org/10.5846/stxb201202290273.

Craig, H. (1961), 1961. Isotopic variations in meteoric waters. Science 133, 1702–1703. https://doi.org/10.1126/science.133.3465.1702.

Cunwei Che, Mingjun Zhang, Athanassios A. Argiriou, Shengjie Wang , Qinqin Du, Peipei Zhao, &Zhuanzhuan Ma, 2019. The Stable Isotopic Composition of DierentWater Bodies at the Soil–Plant–Atmosphere Continuum (SPAC) of the Western Loess Plateau, China. Water 2019 11(9), 1742. https://doi.org/10.3390/w11091742 .

Fan XW, Lin ZJ, Gao ZY, Meng Xiang lian, Niu Fu jun, Luo Jing, Yin Guo an, Zhou Fu jun, &Lan Ai yu, 2021. Cryostructures and ground ice content in ice-rich permafrost area of the Qinghai-Tibet Plateau with Computed Tomography Scanning. Journal of Mountain Science 18(5), 1208-1221. https://doi.org/10.1007/s11629-020-6197-x .

Fu, W., Zhang, X.Y., Zhao, J., Shuli Du, Robert Horton, &Meiting Hou, 2018. Artificial warming-mediated soil freezing and thawing processes can regulate soybean production in Northeast China. Agr. For. Meteorol 262, 249-257. https://doi.org/10.1016/J.AGRFORMET.2018.11.011.

Gaj, M., M. Beyer, P. Koeniger, H. Wanke, J. Hamutoko, &T. Himmelsbach (2016), 2016. In situ unsaturated zone stable water isotope (2H and 18O) measurements: A soil water balance, Hydrology and Earth System Sciences 20(2), 715–731. https://doi.org/10.1016/j.jhydrol.2013.09.006.

Gao Zeyong, Wang Yibo, Liu Guohua, Liu Minghao, Luo Jing, &Yin Jingjing, 2014. Response of soil water in active layer of permafrost area to different alpine ecosystems. Journal of Glaciology and Geocryology 36 (4), 1002-1010.https://doi.org/10.7522/j.issn.1000-0240.2014.0121.

Gibson, J.J., Edwards, T.W.D., Birks, S.J., St Amour, N.A., Buhay, W.M., McEachern, P. McEachern, B. B. Wolfe, D. L. Peters, 2005. Progress in isotope tracer hydrology in Canada. Hydrol. Process 19, 303–327. https://doi.org/10.1002/hyp.5766.

Guo Zhanrong, Jing Enchun, Nie Zhenlong, Jiao Pengcheng, &Dong Hua, 2001. Analysis of soil water movement characteristics during freezing period and freeze-thaw period. Advance in Water Sciences 2002 13 (3), 298-302. https://doi.org/10.3969/j.issn.1001-3946.2001.05.007.

Hongbing Tan, Zihao Lia, Wenbo Raa, Haizhen Wei, Yudong Zhang, &Ben Jin, 2017. Stable isotopes of soil water: Implications for soil water and shallow groundwater recharge in hill and gully regions of the Loess Plateau, China. Agriculture, Ecosystems and Environment 243, 1–9. https://doi.org/10.1016/j.agee.2017.04.001.

Hongbing Tan, Zihao Liu, Wenbo Rao, Haizhen Wei, Yudong Zhang, &Ben Jin, 2017. Stable isotopes of soil water: Implications for soil water and shallow groundwater recharge in hill and gully regions of the Loess Plateau, China. *Agriculture, Ecosystems and Environment 243, 1–9.*

https://doi.org/10.1016/j.agee.2017.04.001.

Hooper, R.P., 2003, 2003. Diagnostic tools for mixing models of stream water chemistry. Water Resour Res 39 (3), 1055. https://doi.org/10.1029/2002wr001528.

Hooper, R.P., Christophersen, N., &Peters, N.E., 1990, 1990. Modelling streamwater chemistry as a mixture of soilwater end-members-an application to the Panola Mountain catchment. Georgia, USA. J. Hydrol 116, 321–343. https://doi.org/10.1016/0022-1694(90)90131-G .

HU Guo-jie, ZHAO Lin, LI Ren, WU Tong-hua, PANG Qiang-qiang, WU Xiao-dong, QIAO Yong-ping, &SHI Jian-zong, 2014. Characteristics of Hydro-thermal Transfer During Freezing and Thawing Period in Permafrost Regions. Soils 46(2), 355–360. https://doi.org/10.13758/j.cnki.tr.2014.02.026.

Hu Hongchang, Wang Genxu, Wang Yibo, Liu Guangsheng, Li Taibing, &Ren Dongxing, 2009. Response of soil heat-water processes to vegetation cover on the typical permafrost and seasonally frozen soil in the headwaters of the Yangtze and Yellow Rivers. Science Bulletin 54(2), 242-250 . https://doi.org/10.1007/s11434-008-0532-x.

Jean C.C. Hsieh, Oliver A. Chadwick, Eugene F. Kelly, &Samuel M. Savin, 1998. Oxygen isotopic composition of soil water:Quantifying evaporation and transpiration. Geoderma 82(1/3), 269–293. https://doi.org/10.1016/S0016-7061(97)00105-5.

Jiao Yongliang, Li Ren, Zhao Lin, Wu Tonghua, Xiao Yao, Hu Guojie, &Qiao Yongping, 2014. Freeze-thaw status of active layer and characteristics of soil water transport in permafrost area. Journal of Glaciology and Geocryology 36(2), 237-247. https://doi.org/10.7522/j.issn.1000-0240.2014.0030.

https://doi.org/10.5194/hess-2021-558
Preprint. Discussion started: 8 November 2021

Jinzhao Liu, Huawu Wu, Yao Cheng, Zhao Jin, &Jing Hu， 2021. Stable isotope analysis of soil and plant water in a pair of natural grassland and understory of planted forestland on the Chinese Loess Plateau. Agricultural Water Management 249. https://doi.org/10.1016/j.agwat.2021.106800.

Kanevskiy, M., Jorgenson, T., Shur, Y., O’Donnell, J.A., Harden, J.W., Zhuang, Q., &Fortier, D, 2014. Cryostratigraphy and permafrost evolution in the lacustrine lowlands of westcentral Alaska. Permafr. Periglac. Process 25 (1), 14–34. https://doi.org/10.1002/ppp.1800 .

Klaus, J., and J. McDonnell (2013), 2013. Hydrograph separation using stable isotopes: Review and evaluation. J. Hydrol., 505, 47–64, https://doi.org/10.1016/j.jhydrol.2013.09.006.

L. Aragufis-Aragufis, K. Rozanski, R. Gonfiantini, &D. Louvat, 1995. Isotope effects accompanying vacuum extraction of soil water for stable isotope analyses. Journal of Hydrology 168 (1), 159-171. https://doi.org/10.1016/0022-1694(94)02636-P.

Landwehr, J. M., & Coplen, T. B., 2012.Line-conditioned excess: A new method for characterizing stable hydrogen and oxygen isotope ratios in hydrologic systems. Paper presented at the International Conference on Isotopes in Environmental Studies, (pp. 132–135). Vienna, International Atomic Energy Agency.

Landwehr, J. M., Coplen, T. B., & Stewart, &D. W. (2014), 2014. Spatial, seasonal,and source variability in the stable oxygen and hydrogen isotopic composition of tap waters throughout the USA. Hydrological Processes 28(21), 5382–5422. https://doi.org/10.1002/hyp.10004.

Li Yuanshou, Wang Genxu, Zhao Lin, Wu Qingbai, Wang Yibo, &Zhang Renhe, 2010. Response of soil water in permafrost active layer of Qinghai-Tibet Plateau to

https://doi.org/10.5194/hess-2021-558
Preprint. Discussion started: 8 November 2021

alpine meadow cover change. Journal of Glaciology and Geocryology 32 (1), 157-165. http://ir.casnw.net/handle/362004/8479.

LI Yuan-shou, WANG Gen-xu, ZHAO Lin, WU Qing-bai,□WANG Yi bo, &ZHANG Ren-he. : Response of Soil water in the Permafrost Active Layer to the Change of Alpine Meadow Coverage on the Tibetan Plateau. Journal of Glaciology and Geocryology, 32(1), 157-165.

Li Zongxing, Li Zongjie, Feng Qi, Zhang Baijuan, Gui Juan, Xue Jian, &Gao Wende, 2020.

Runoff dominated by supra-permafrost water in the source region of the Yangtze river using environmental isotopes. Journal of Hydrology 582, 1-20. https://doi.org/10.1016/j.jhydrol.2019.124506.

Li, Z.-X., Feng, Q., Liu, W., Wang, T.-T., Chen, A.-F., Gao, Y., Guo Xiaoyan, Pan Yanhui, Li Jianguo, Guo Rui, &Jia Bing, 2014. tudy on the contribution from cryosphere to runoff in the cold Alpine Basin: a case study of Hulugou River Basin in the Qilian Mountains. Glob. Plane, Chan 122, 345–361. https://doi.org/10.1016/j.gloplacha.2014.10.001.

Liu Jinzhaoa, Huawu Wu, Yao Cheng, Zhao Jin, &Jing Hu, 2021. Stable isotope analysis of soil and plant water in a pair of natural grassland and understory of planted forestland on the Chinese Loess Plateau. *Agricultural Water Management 249,1-9.* https://doi.org/10.1016/j.agwat.2021.106800.

Liu, G.S., Wang, G.X., Hu, C.H., LI Tai-bingWANG, Jun-fengREN, Dong-xingHUANG, &Ya-juan. : Influence of vegetation coverage on water and heat processes of the active layer in permafrost regions of the Tibetan Plateau. J. Glaciol, Geocryol 31 (1), 89-95.

Matthias Sprenger, Doerthe Tetzlaff, &Chris Soulsby, 2017. Soil water stable isotopes

https://doi.org/10.5194/hess-2021-558
Preprint. Discussion started: 8 November 2021

reveal evaporation dynamics at the soil–plant–atmosphere interface of the critical zone. Hydrology and Earth System Sciences 21, 3839–3858, http://doi.org /10.5194/hess-21-3839-2017.

Matthias Sprenger, Doerthe Tetzlaff, and Chris Soulsby, 2017. Soil water stable isotopes reveal evaporation dynamics at the soil–plant–atmosphere interface of the critical zone. Hydrol. Earth Syst. Sci. 21, 3839–3858. https://doi.org/10.5194/hess-21-3839-2017 .

Niu, F.J., Gao, Z.Y., Lin, Z.J., Luo Jing, &Fan Xingwen, 2019. Vegetation influence on the soil hydrological regime in permafrost regions of the Qinghai-Tibet Plateau,China. Geoderma 354, 1-11. https://doi.org/10.1016/j.geoderma.2019.113892 .

Peng Wang, Judith de Jager, Ake Nauta, Jacobus van Huissteden, Maximov C. Trofim, &Juul Limpens, 2019. Exploring near-surface ground ice distribution in patterned-ground tundra: correlations with topography, soil and vegetation. Plant Soil 444(1-2), 251–265. https://doi.org/10.1007/s11104-019-04276-7 .

Phillips DL, &Gregg JW, 2003. Source partitioning using stable isotopes: coping with too many sources. Oecologia 136, 261-269. https://doi.org/10.1007/s00442-003-1218-3.

Schuur, E.A.G., Mack, M.C., 2018, 2018. Ecological response to permafrost thaw and consequences for local and global ecosystem services. Annu. Rev. Ecol. Evol. Syst 49, 279-301. https://doi.org/10.1146/annurev-ecolsys-121415-032349.

Sprenger, M., H. Leistert, K. Gimbel, & M. Weiler (2016), 2016. Illuminating hydrological processes at the soil-vegetation-atmosphere interface with water

https://doi.org/10.5194/hess-2021-558
Preprint. Discussion started: 8 November 2021

Hydrology and Earth System Sciences
Discussions

stableisotopes.Rev.Geophys 54(3),674-704. https://doi.org/10.1002/2015RG000515.

Sprenger, M., H. Leistert, K. Gimbel,& M.Weiler (2016) , 2016. Illuminating hydrological processes at thesoil-vegetation-atmosphere interface with water stable isotopes. Rev.Geophys 54(3), 674-704. https://doi.org/10.1002/2015RG000515.

Wang, P., X. Song, D. Han, Y. Zhang, and X. Liu (2010), 2010. A study of root water uptake of crops indicated by hydrogen and oxygen stable isotopes: A case in Shanxi Province, China, Agr. Water Manag. 97(3), 475–482. https://doi.org/10.1016/j.agwat.2009.11.008.

WU Xiaoli, LIU Guimin1, LI Xinxing, JI Genghao, LI Lisha1, MAO Nan, XU Haiyan, &WU Xiaodong, 2021. Variation of Soil water and Its Relation with Precipitation of Permafrost and Seasonally Frozen Soil Regions on the Qinghai-Tibet Plateau. Journal of China Hydrology 41(1),73-101. https://doi.org/10.19797/j.cnki.1000-0852.20190430 .

Wu, P., Liang, S.H., Wang, X.S., Yuqing Feng, &Jeffrey M. McKenzie, 2018. A new assessment of hydrological change in the Source Region of the Yellow River. Water 10(7), 877. https://doi.org/10.1023/A:1024458411589.

Yang, K., &Wang, C.H., 2019. Water storage effect of soil freeze-thaw process and its impacts on soil hydro-thermal regime variations. Agr For Meteorol 265, 280-294.

Yang, Z., Gao, J., Zhao, L., Xing-liang Xu, &Hua Ouyang, 2013. Linking thaw depth with soil water and plant community composition: effects of permafrost

https://doi.org/10.5194/hess-2021-558
Preprint. Discussion started: 8 November 2021

degradation on alpine ecosystems on the Qinghai-Tibet Plateau. Plant Soil 367, 687-700.https://doi.org/10.1007/s11104-012-1511-1.

Youjie Wu, Taisheng Du, Risheng Ding, Yusen Yuan, Sien Li,&Ling Tong, 2017. An isotope method to quantify soil evaporation and evaluate watervapor movement under plastic film mulch. Agricultural Water Management 184, 59–66. https://doi.org/10.1016/j.agwat.2017.01.005.

Yuhong Liu, Fude Liu, Zhen Xu, Jianping Zhang, LixinWang, &Shuqing An, 2015. Variations of soil water isotopes and effective contribution times of precipitation and throughfall to alpine soil water, in Wolong Nature Reserve, China. Catena 126, 201–208. https://doi.org/10.1016/j.catena.2014.11.008.

Yuhong Liu, Zhen Xu, Rodney Duffy, Wenlian Chen, Shuqing An, Shirong Liu, &Fude Liu. Analyzing relationships among water uptake patterns, rootlet biomass distribution and soil water content profile in a subalpine shrubland using water isotopes. European Journal of Soil Biology 47(6), 380-386. https://doi.org/10.1016/j.ejsobi.2011.07.012.

ZHU Meizhuang，WANG Genxu，XIAO Yao，HU Zhaoyong, SONG Chunlin, &HUANG Kewei, 2017．A study on the changes of soil water infiltration in alpine meadow of permafrost regions in the Tibetan Plateau． Journal of Glaciology and Geocryology 39(6), 1316 – 1325． https://doi.org/10.7522/j.issn.1000-0240.2017.0324.

Zimmermann, U., K. O. Münnich, W. Roether, W. Kreutz, K. Schubach, and O. Siegel (1966), 1966. Tracers determine movement of soil water and Evapotranspiration. Science 152(3720), 346–347. https://doi.org/10.1126/science.152.3720.346.

https://doi.org/10.5194/hess-2021-558
Preprint. Discussion started: 8 November 2021

Zongjie Li, Jinzhu Ma, Lingling Song, Juan Gui, Jian Xue, Baijuan Zhang, Wende Gao,&ZZongxing Li, 2020. Investigation of soil water hydrological process in the permafrost active layer using stable isotopes. Hydrological Processes 34(12), 1–13. https://doi.org/10.1002/hyp.13765.

Tables:

Table.1 Relationship between $\delta^{18}O$ and d-excess, EL for soil waters in study region

Table.2 Correlation between soil water stable isotopes and soil moisture in study region

Table.3 Correlation between soil water stable isotopes and soil temperature in study region

Table.1 Relationship between $\delta^{18}O$ and d-excess, EL for soil waters in study region

	Relationship between $\delta^{18}O$ and d-excess/ R^2	EL/ R^2
All soil water samples	$Y=-0.16x+3.87$, $R^2=0.0065$	
0-20cm	$Y=-0.43x+0.98$, $R^2=0.065$	
20-40cm	$Y=-0.4564x+0.7948$, $R^2=0.0392$	
40-60cm	$Y=-1.05x-7.33$, $R^2=0.1667$	
60-80cm	$Y=-0.32x+2.5781$, $R^2=0.0167$	

https://doi.org/10.5194/hess-2021-558
Preprint. Discussion started: 8 November 2021

Hydrology and Earth System Sciences
Open Access
Discussions

80-100cm	Y=-1.1944x-7.3393, R^2=0.1584	
Sunny slope	Y=-0.7x-2.2479, R^2=0.0956	$\delta^2H = 7.28\delta^{18}O - 2.58$ R^2=0.92
Shady slope	Y=-0.4337x+0.8866, R^2=0.0543	$\delta^2H = 7.56\delta^{18}O + 0.77$ R^2=0.95
Grassland	Y=-0.4921x-0.5722, R^2=0.0715	$\delta^2H = 7.50\delta^{18}O - 0.80$ R^2=0.95
Meadow	Y=-0.6067x+0.8133, R^2=0.0615	$\delta^2H = 7.38\delta^{18}O + 0.67$ R^2=0.91
Forest	Y=-1.4013x-12.706, R^2=0.2283	$\delta^2H = 6.44\delta^{18}O - 14.97$ R^2=0.85

Table.2 Correlation between soil water stable isotopes and soil moisture in study region

Types	Relationship between $\delta^{18}O$ and soil moisture/R^2	Relationship between d-excess and soil moisture/R^2	Soil moisture
0-20cm	$\delta^{18}O$ = -0.084H -7.8 R^2=0.08	D-excess = 0.14H +0.54 R^2=0.08	35.58 %
20-40cm	$\delta^{18}O$ = -0.046H -9.93 R^2=0.02	D-excess = 0.095H +2.54 R^2=0.01	36.62 %
40-60cm	$\delta^{18}O$ = -0.022H -11.91 R^2=-0.01	D-excess = 0.36H -6.38 R^2=0.01	34.82%
60-80cm	$\delta^{18}O$ =0.01H -14.38 R^2=0.001	D-excess = 0.54H -10.14 R^2=0.54	32.04%

https://doi.org/10.5194/hess-2021-558
Preprint. Discussion started: 8 November 2021

80-100cm	$\delta^{18}O$ =-0.008H -10.79 R^2=0.002	D-excess = 0.15H+0.59 R^2=0.09	35.55%
Grassland	$\delta^{18}O$ =-0.055H -9.59 R^2=0.03	D-excess = 0.13H+0.89 R^2=0.04	36.78%
Meadow	$\delta^{18}O$ =-0.024H -10.64 R^2=0.01	D-excess = 0.2H+0.12 R^2=0.12	32.91%
Frost	$\delta^{18}O$ =-0.07H -10.25 R^2=0.05	D-excess = 0.53H-14.49 R^2=0.3	33.36%
Shady slope	$\delta^{18}O$ =-0.084H -8.43 R^2=0.06	D-excess = 0.22H-1.67 R^2=0.12	34.68%
Sunny slope	$\delta^{18}O$ =-0.011H -11.42 R^2=0.0019	D-excess = 0.145H+0.82 R^2=0.06	35.94%

Table.3 Correlation between soil water stable isotopes and soil temperature in study region

Types	Relationship between $\delta^{18}O$ and soil temperature/R^2	Relationship between d-excess and soil temperature/R^2	Soil temperature
0-20cm	$\delta^{18}O$ = -0.21T -7.3 R^2=0.08	D-excess = -0.34T +11.3 R^2=0.08	16.43°C
20-40cm	$\delta^{18}O$ = 0.09T -12.01 R^2=0.016	D-excess = -0.81T +16.34 R^2=0.24	13.09°C
40-60cm	$\delta^{18}O$=0.007H	D-excess =-0.73H	11.33°C

https://doi.org/10.5194/hess-2021-558
Preprint. Discussion started: 8 November 2021

	-12.79 R^2=-0.017	+14.36 R^2=0.13	
60-80cm	$\delta^{18}O$ =-0.04H -13.59 R^2=0.003	D-excess = -0.72H +15.36 R^2=0.16	11.18°C
80-100cm	$\delta^{18}O$ =-0.15H -9.48 R^2=0.04	D-excess =-0.76H+14.28 R^2=0.12	10.95 °C
Grassland	$\delta^{18}O$ =-0.04H -10.77 R^2=0.002	D-excess = -0.469H+11.43 R^2=0.11	13.91°C
Meadow	$\delta^{18}O$ =0.12H -13.11 R^2=0.04	D-excess = -0.46H+13.54 R^2=0.10	12.17°C
Frost	$\delta^{18}O$ =0.14H -15.28 R^2=0.08	D-excess = -0.67H+16.88 R^2=0.21	14.69°C
Shady slope	$\delta^{18}O$=0.0098H -11.35 R^2=-0.006	D-excess =-0.47H+12.08 R^2=0.12	13.73°C
Sunny slope	$\delta^{18}O$=-0.0039H -11.77 R^2=-0.007	D-excess = -0.51H+12.96 R^2=0.13	13.57°C

Figures

Fig.1 The location of Three-River Headwater Region and distribution of sampling sites for soils and waters

Fig.2 Photograph of permafrost ground ice in the study region

https://doi.org/10.5194/hess-2021-558
Preprint. Discussion started: 8 November 2021

Hydrology and Earth System Sciences Discussions

Fig.3 Plot of δD versus $\delta^{18}O$ and EL for soil water in different soil layers and sources region

Fig.4 Variation of $\delta^{18}O$ and d-excess with soil profile

Fig.5 Spatial pattern of $\delta^{18}O$ for different soil layers

Fig.6 Spatial pattern of d-excess for different soil layers

Fig.7 Variation of Ic-excess with soil profile

Fig.8 The plot of δD versus $\delta^{18}O$ for different waters in study region (a), different altitude (b), different vegetation (c), different slope (d)

Fig.9. Two end element diagram using the mean values of $\delta^{18}O$ and δD for soil water

Fig.10 Contribution from precipitation and ground ice to soil water in different soil layers (a), different altitudes (b), different vegetation (c), and sunny slope and shady slope (d)

Fig.11 Altitude effect of $\delta^{18}O$ and d-excess for soil water in the whole study region (a), grassland (b) and meadow (c)

Fig.12 Correlation between stable isotope and soil moisture (a), and soil temperature (b)

Fig.13 Correlation between stable isotope and vegetation cover (a), grass height (b), and root depth (c)

Fig.14 Ecological protection for vegetation degradation caused by the decreasing soil water in permafrost active layer

https://doi.org/10.5194/hess-2021-558
Preprint. Discussion started: 8 November 2021

Hydrology and Earth System Sciences
Discussions

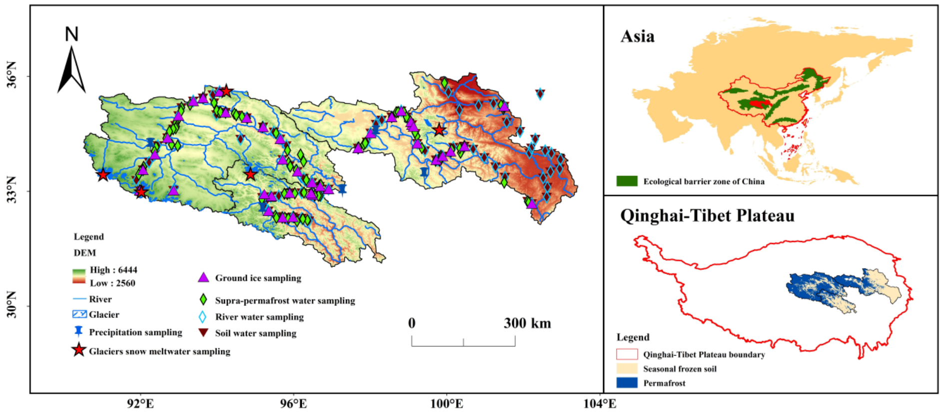

Fig.1

Fig. 2

https://doi.org/10.5194/hess-2021-558
Preprint. Discussion started: 8 November 2021

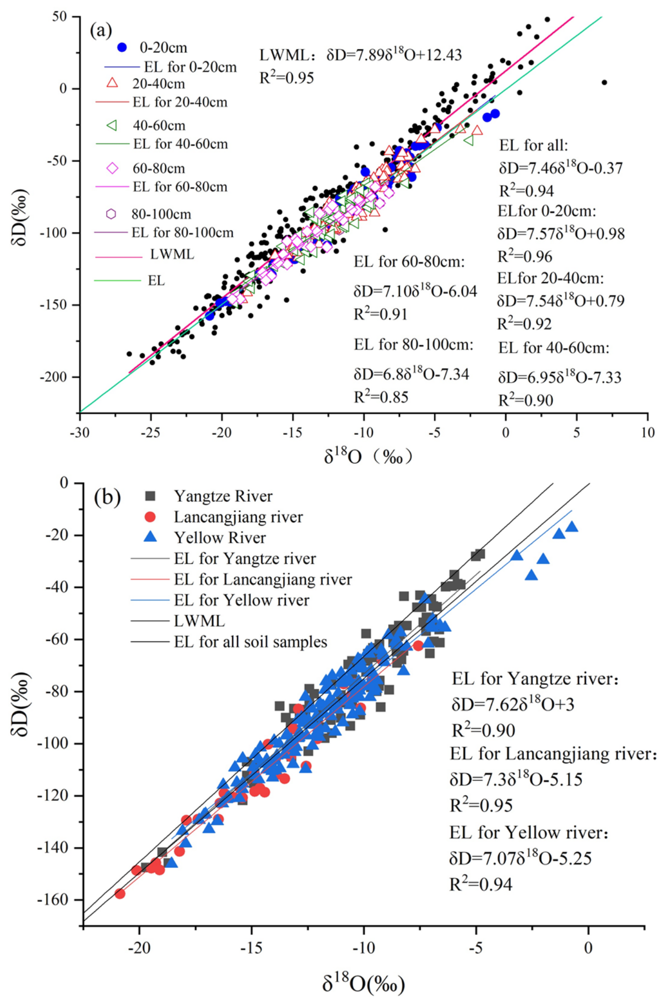

1309

1310 Fig.3

https://doi.org/10.5194/hess-2021-558
Preprint. Discussion started: 8 November 2021

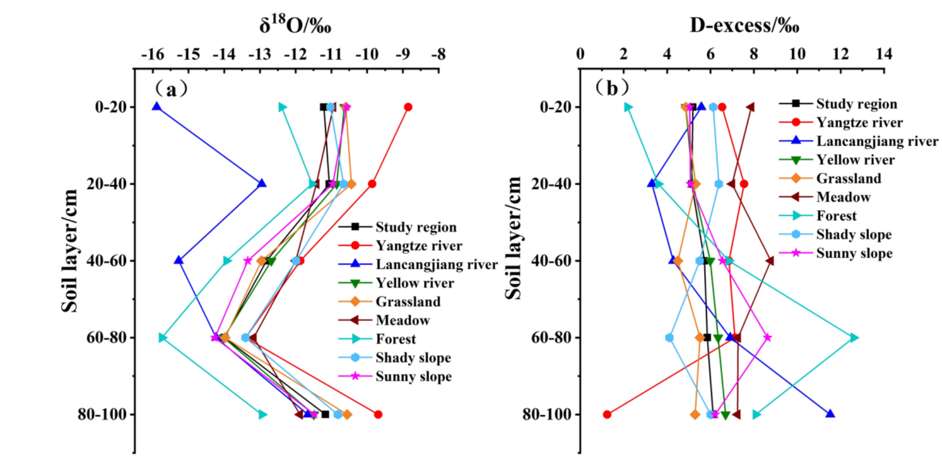

Fig.4

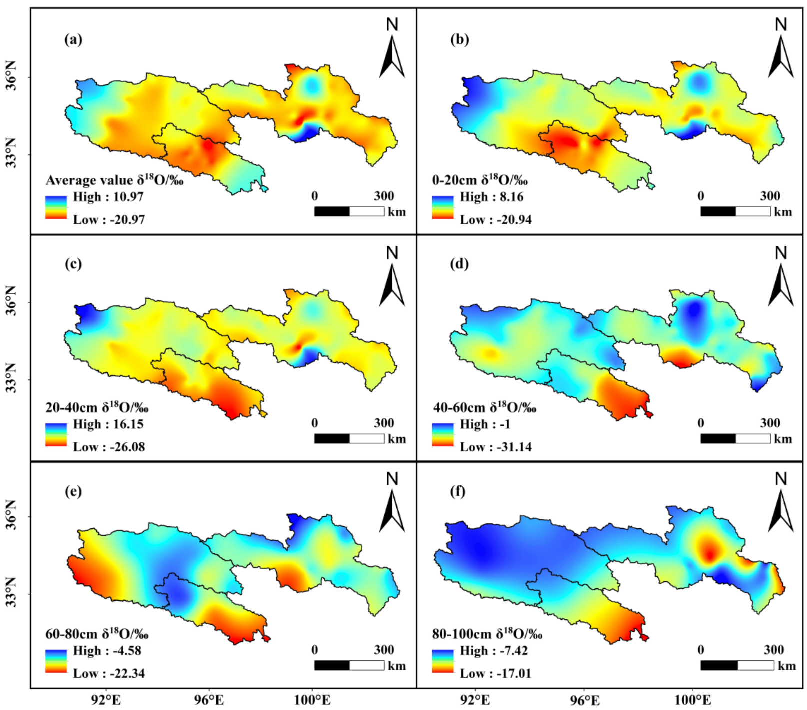

Fig.5

https://doi.org/10.5194/hess-2021-558
Preprint. Discussion started: 8 November 2021

Hydrology and Earth System Sciences
Discussions

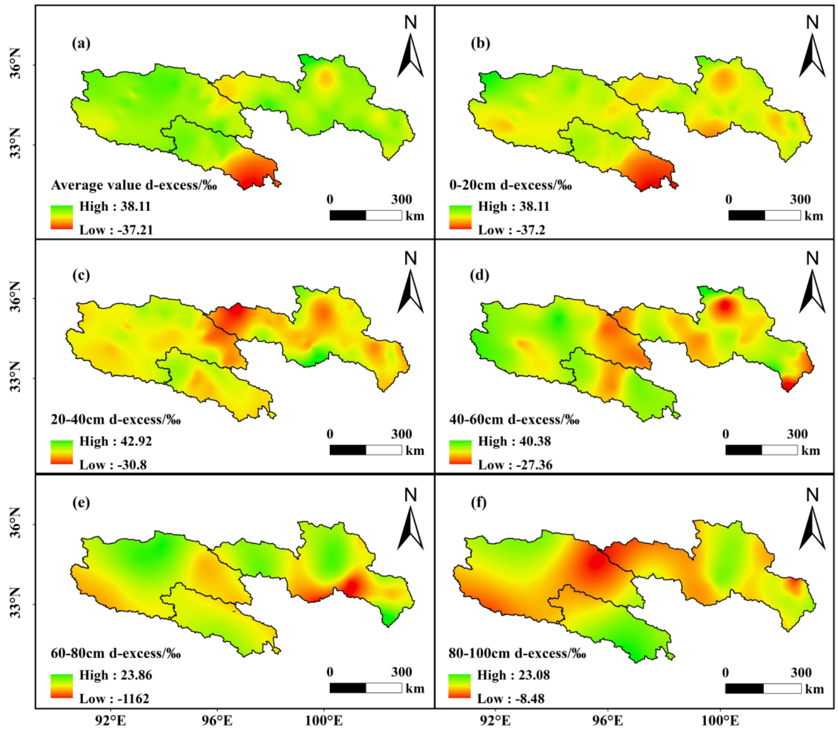

1315

1316 Fig.6

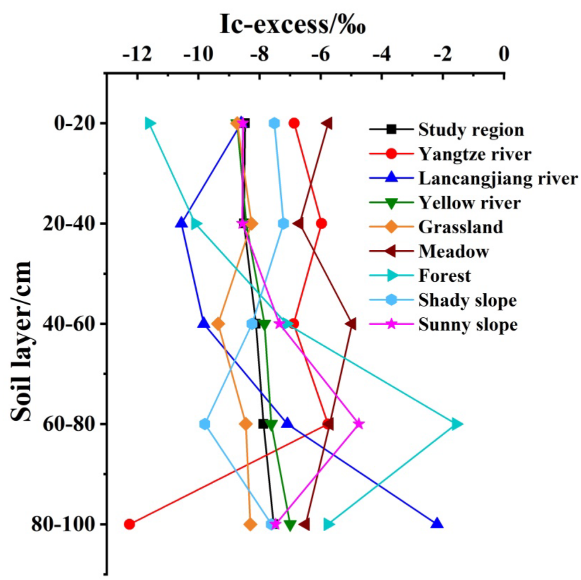

1317

1318 Fig.7

https://doi.org/10.5194/hess-2021-558
Preprint. Discussion started: 8 November 2021

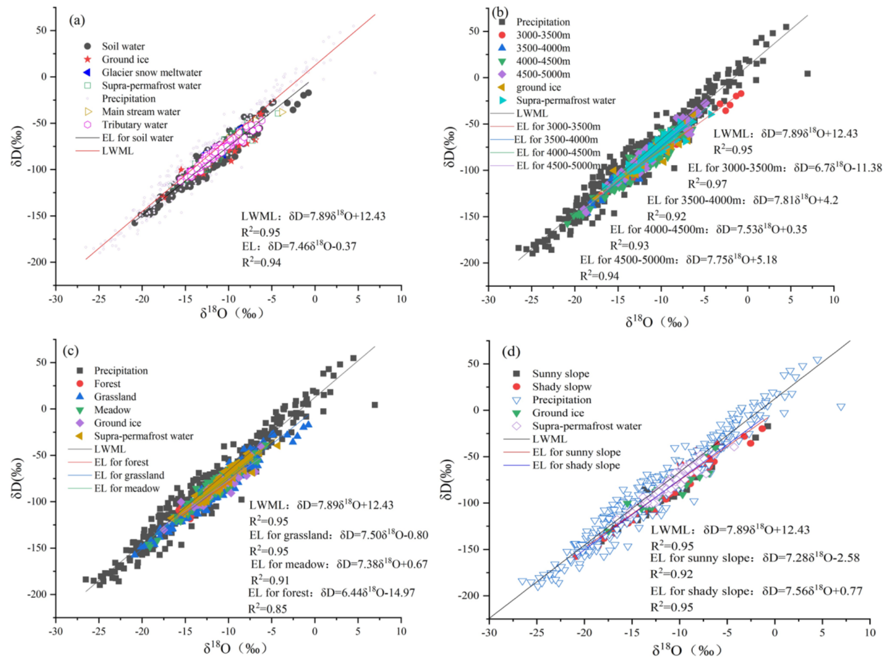

Fig.8

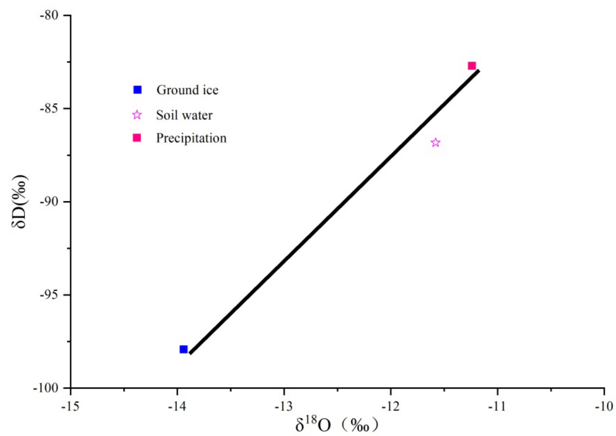

Fig.9

https://doi.org/10.5194/hess-2021-558
Preprint. Discussion started: 8 November 2021

Hydrology and Earth System Sciences
Open Access
Discussions

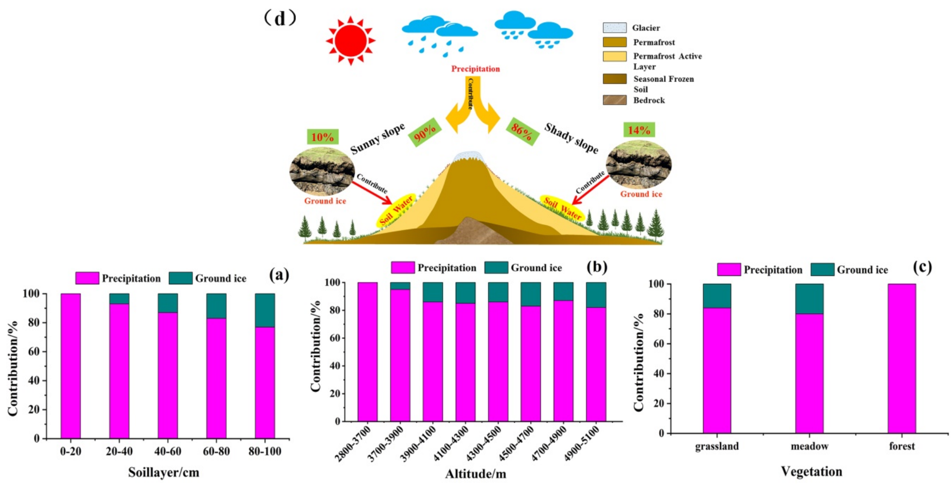

1323

1324 Fig.10

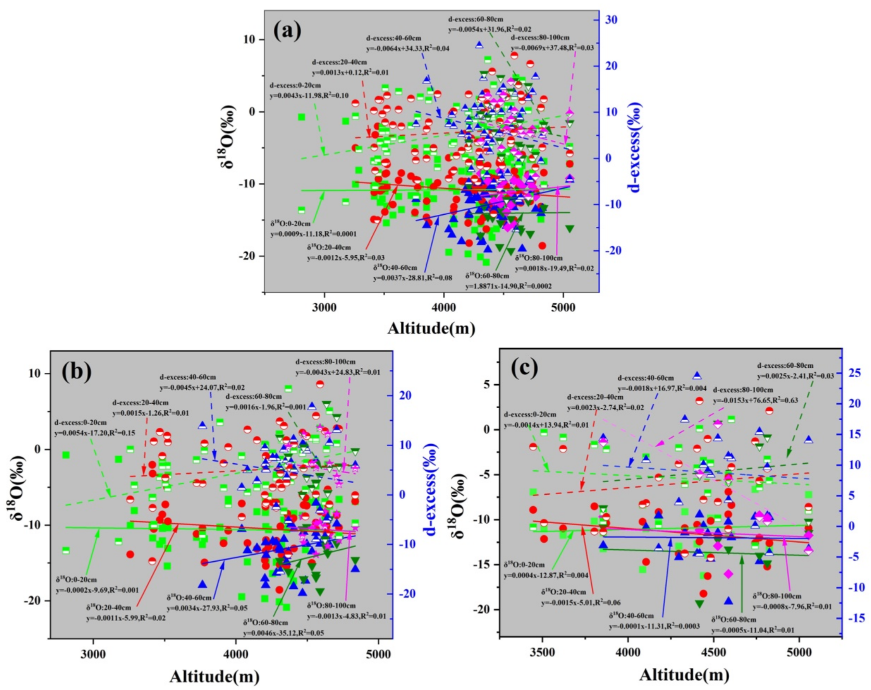

1325

1326 Fig.11

https://doi.org/10.5194/hess-2021-558
Preprint. Discussion started: 8 November 2021

Hydrology and Earth System Sciences
Open Access
Discussions

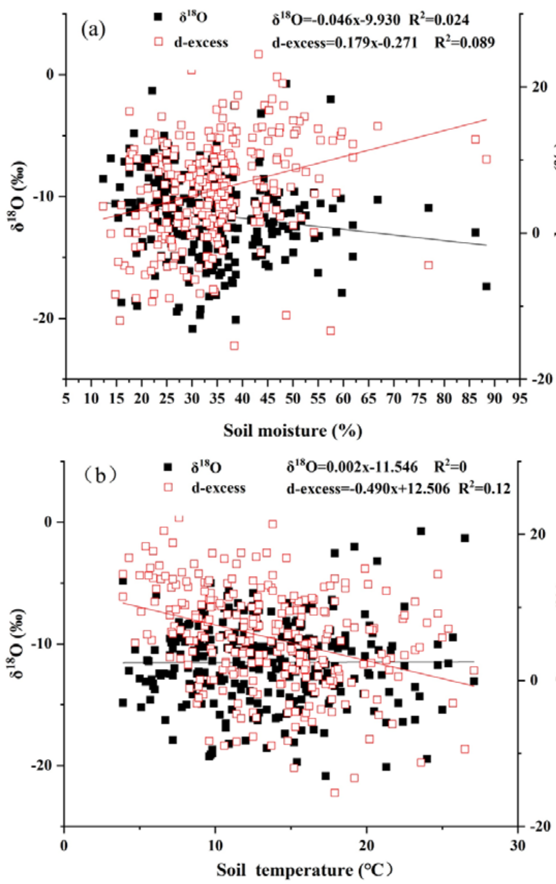

1327

1328 Fig.12

https://doi.org/10.5194/hess-2021-558
Preprint. Discussion started: 8 November 2021

Hydrology and Earth System Sciences
Discussions

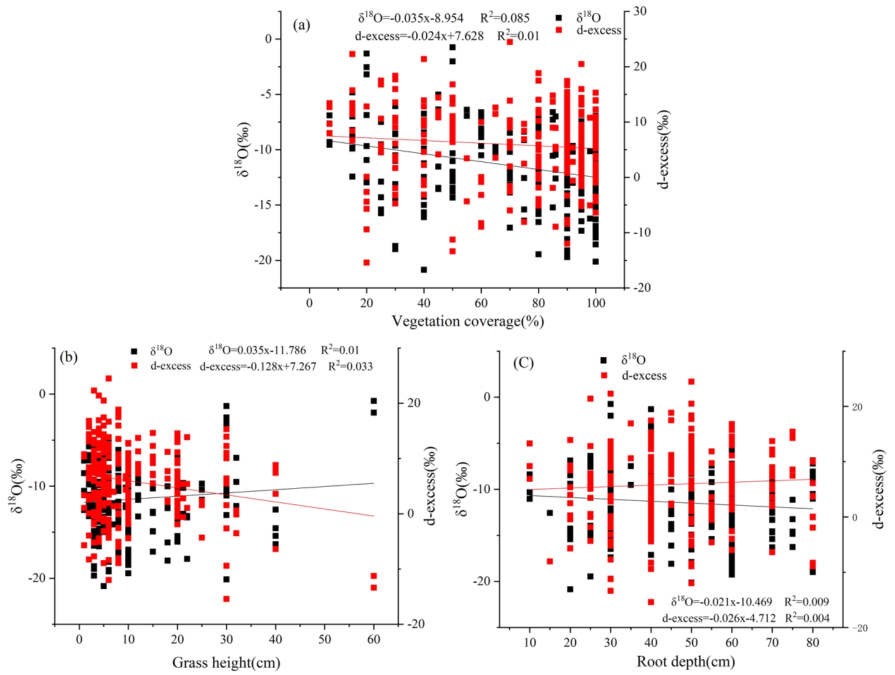

Fig.13

https://doi.org/10.5194/hess-2021-558
Preprint. Discussion started: 8 November 2021

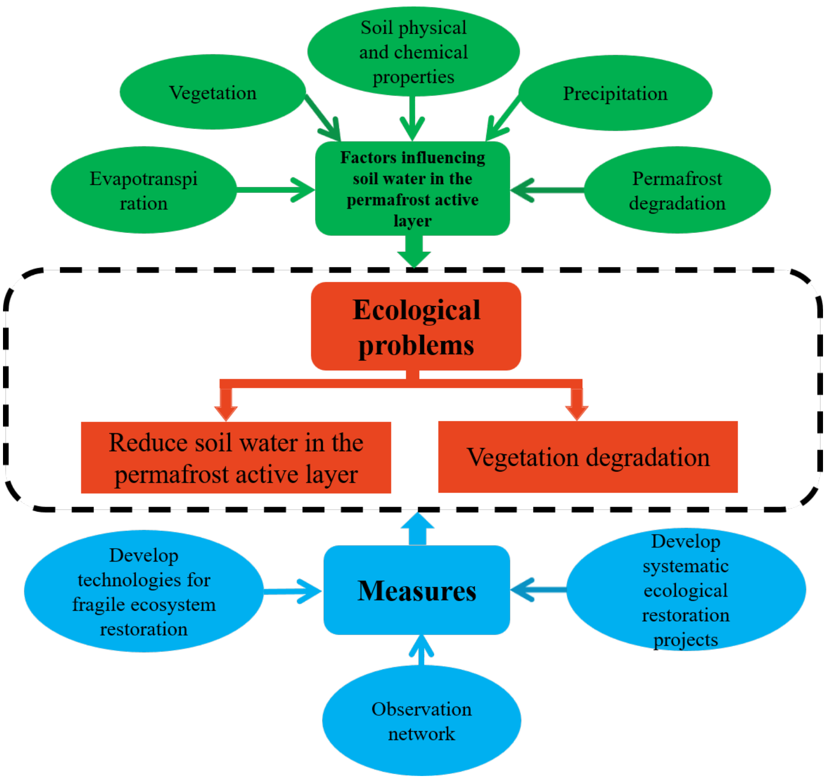

1332 Fig.14